**Fig. 2.** Field emission scanning electron microscopy (FESEM) of cerebellar granular neurons exposed to taipoxin (6 nM for 60 min) or mLysoPC+OA (30 μM for 15 min) at lower (left panels) and higher (right panels) magnifications (**A**). Identical results were obtained with notexin, β-bungarotoxin, and textilotoxin. Scale bar, 10 μm (left panels) and 2 μm (right panels). (**B**) Cerebellar neurons were exposed to 6 nM β-bungarotoxin for 60 min or to 30 μM mLysoPC+OA for 15 min and stained with an antibody specific for the lumenal domain of synaptotagmin I before fixation. Samples were processed for indirect immunofluorescence without permeabilization; superimposable results were obtained with notexin, taipoxin, and textilotoxin in cerebellar neurons and hippocampal neurons. Scale bar, 10 μm.
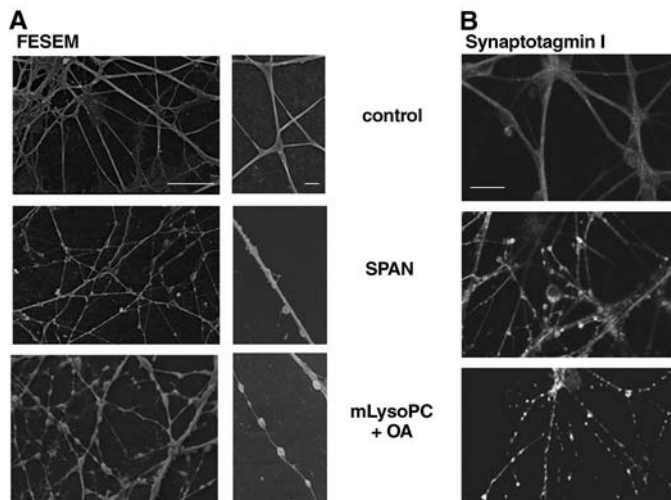
ment of PLA2 in other exocytotic events such as the sperm acrosomal exocytosis (*24*). Furthermore, a SPAN microinjected into pheochromocytoma cells inhibited neuroexocytosis (*25*), presumably because it acted on the cytosolic plasma membrane side, inducing an opposite membrane configuration. The presence of clathrin-coated Ω-shaped structures in SPAN-poisoned NMJs (*4–7*) suggested that they also inhibit synaptic vesicle fission from the plasma membrane (*3, 14*). Indeed, the same SPAN-induced lipid changes promoting membrane fusion do inhibit membrane fission for the same physical and topological reasons (*17*).

References and Notes

1. R. M. Kini, Ed., *Venom Phospholipase A2 Enzymes* (Wiley, Chichester, UK, 1997).
2. G. Schiavo, M. Matteoli, C. Montecucco, *Physiol. Rev.* **80**, 717 (2000).
3. C. Montecucco, O. Rossetto, *Trends Biochem. Sci.* **25**, 266 (2000).
4. S. G. Cull-Candy, J. Fohlman, D. Gustavsson, R. Lullmann-Rauch, S. Thesleff, *Neuroscience* **1**, 175 (1976).
5. I. L. Chen, C. Y. Lee, *Virchows Arch. B Cell Pathol.* **6**, 318 (1970).
6. J. B. Harris, B. D. Grubb, C. A. Maltin, R. Dixon, *Exp. Neurol.* **161**, 517 (2000).
7. C. Y. Lee, M. C. Tsa, Y. M. Chen, A. Ritonja, F. Gubensek, *Arch. Int. Pharmacodyn. Ther.* **268**, 313 (1984).
8. P. Rosenberg, *Venom Phospholipase A2 Enzymes*, R. M. Kini, Ed. (Wiley, Chichester, UK, 1997), pp. 155-183.
9. R. M. Kini, *Toxicon* **42**, 827 (2003).
10. C. C. Yang, in *Venom Phospholipase A2 Enzymes*, R. M. Kini, Ed. (Wiley, Chichester, UK,1997), pp. 185-204.
11. R. E. Stafford, T. Fanni, E. A. Dennis, *Biochemistry* **28**, 5113 (1989).
12. J. Wang *et al.*, *Br. J. Pharmacol.* **141**, 586 (2004).
13. M. Rigoni *et al.*, *J. Cell Sci.* **15**, 3561 (2004).
14. D. Bonanomi *et al.*, *Mol. Pharmacol.* **67**, 1901 (2005).
15. F. Kamp, D. Zakim, F. Zhang, N. Noy, J. A. Hamilton, *Biochemistry* **34**, 11928 (1995).
16. L. V. Chernomordik, E. Leikina, V. Frolov, P. Bronk, J. Zimmerberg, *J. Cell Biol.* **136**, 81 (1997).
17. L. V. Chernomordik, M. M. Kozlov, *Annu. Rev. Biochem.* **72**, 175 (2003).
18. Y. Xu, F. Zhang, Z. Su, J. A. McNew, Y. K. Shin, *Nat. Struct. Mol. Biol.* **12**, 417 (2005).
19. C. G. Giraudo *et al.*, *J. Cell Biol.* **170**, 249 (2005).
20. C. Reese, F. Heise, A. Mayer, *Nature* **436**, 410 (2005).
21. K. Farsad, P. De Camilli, *Curr. Opin. Cell Biol.* **15**, 372 (2003).
22. R. Jahn, T. Lang, T. C. Sudhof, *Cell* **112**, 519 (2003).
23. L. K. Tamm, J. Crane, V. Kiessling, *Curr. Opin. Struct. Biol.* **13**, 453 (2003).
24. E. R. S. Roldan, *Front. Biosci.* **3**, 1119 (1998).
25. S. Wei *et al.*, *Neuroscience* **121**, 891 (2003).
26. Supported by Telethon grant GP0272Y01, COFIN Project 2002055747, FISR-DM 16/10/00, FIRB-RBNE01RHZM, University of Padova, and Cancer Research UK.

Neural Systems Responding to Degrees of Uncertainty in Human Decision-Making

Ming Hsu,[1] Meghana Bhatt,[1] Ralph Adolphs,[1,2] Daniel Tranel,[2] Colin F. Camerer[1]*

Much is known about how people make decisions under varying levels of probability (risk). Less is known about the neural basis of decision-making when probabilities are uncertain because of missing information (ambiguity). In decision theory, ambiguity about probabilities should not affect choices. Using functional brain imaging, we show that the level of ambiguity in choices correlates positively with activation in the amygdala and orbitofrontal cortex, and negatively with a striatal system. Moreover, striatal activity correlates positively with expected reward. Neurological subjects with orbitofrontal lesions were insensitive to the level of ambiguity and risk in behavioral choices. These data suggest a general neural circuit responding to degrees of uncertainty, contrary to decision theory.

In theories of choice under uncertainty used in social sciences and behavioral ecology, the only variables that should influence an uncertain choice are the judged probabilities of possible outcomes and the evaluation of those outcomes. But confidence in judged probability can vary widely. In some choices, such as gambling on a roulette wheel, probability can be confidently judged from relative frequencies, event histories, or an accepted theory. At the other extreme, such as the chance of a terrorist attack, probabilities are based on meager or conflicting evidence, where important information is clearly missing. The two types of uncertain events are often called risky and ambiguous, respectively. In subjective expected utility theory, the probabilities of outcomes should influence choices, whereas confidence about those probabilities should not. But experiments show that many people are more willing to bet on risky outcomes than on ambiguous ones, holding judged probability of outcomes constant (*1*). This empirical aversion to ambiguity motivates a search for neural distinctions between risk and ambiguity. Here, we extend the study of the neural basis of decision under risk to encompass ambiguity.

The difference between risky and ambiguous uncertainty is illustrated by the Ellsberg paradox (*2*). Imagine one deck of 20 cards composed of 10 red and 10 blue cards (the risky deck). Another deck has 20 red or blue cards, but the composition of red and blue cards is completely unknown (the ambiguous deck). A bet on a color pays a fixed sum (e.g., $10) if a card with the chosen color is drawn, and zero otherwise (Fig. 1A).

[1]Division of Humanities and Social Sciences, 228-77, California Institute of Technology, Pasadena, CA 91125, USA. [2]University of Iowa Medical School, Iowa City, IA 52242, USA.

*To whom correspondence should be addressed. E-mail: camerer@hss.caltech.edu

A Card-Deck

B Knowledge

C Informed Opponent
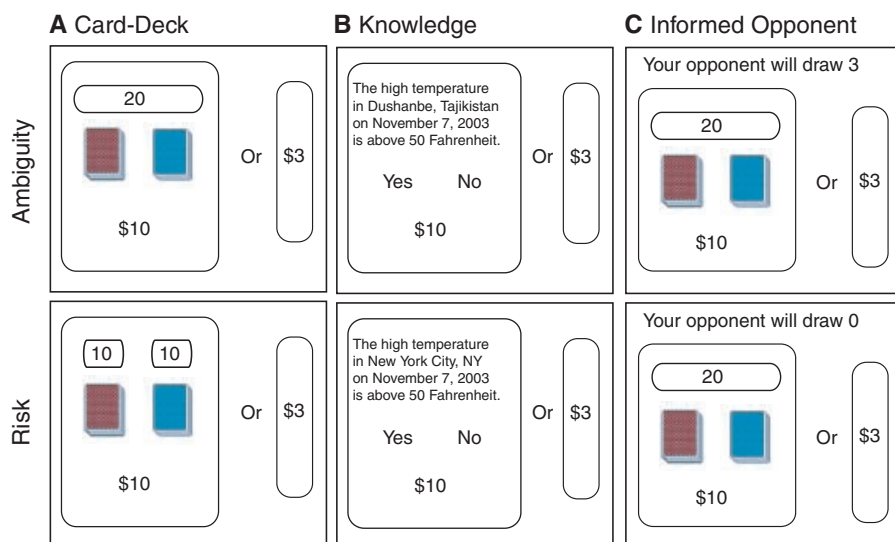
Fig. 1. Sample screens from the experiment. The conditions in the top panel are called ambiguous because the subject is missing relevant information that is available in the risk conditions (bottom panel). Subjects always choose between betting on one of the two options on the left side or taking the certain payoff on the right. (**A**) Card-Deck treatment: Ambiguity is not knowing the exact proportion; risk is knowing the number of cards (indicated by numbers above each deck). (**B**) Knowledge treatment: Ambiguity is knowing less about the uncertain events (e.g., Tajikistan) relative to risk (e.g., New York City). (**C**) Informed Opponent treatment: Ambiguity is betting against an opponent who has more information (who drew a three-card sample from the deck) than in risk (where the opponent drew no cards from the deck). Bets win if subject chooses the realized color and opponent chooses the opposite color; otherwise, both take the certain payoff [see (17)].
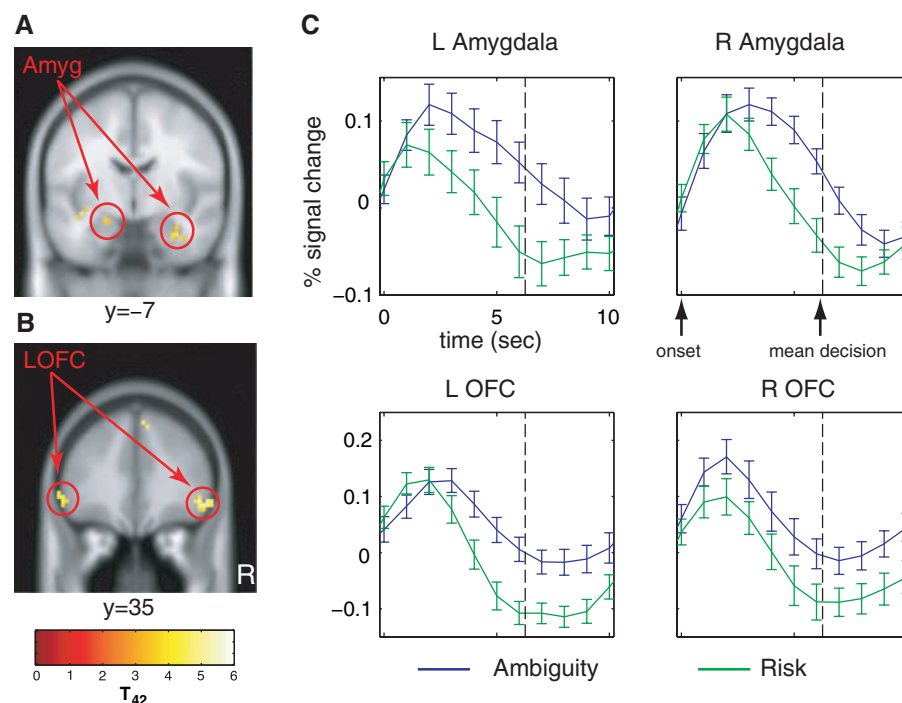
Fig. 2. Regions showing greater activation in response to ambiguity than in response to risk. Random-effects analysis of all three treatments revealed regions that are differentially activated in decision-making under ambiguity relative to risk ($P \leq 0.001$, uncorrected; cluster size $k \geq 10$ voxels). These regions include (**A**) left amygdala and right amygdala/parahippocampal gyrus (coronal section shown at $y = 7$ in MNI space; heat map represents t statistic with 42 degrees of freedom) and (**B**) bilateral OFC. (**C**) Mean time courses of amygdala and OFC (time synched to trial onset, dashed vertical lines are mean decision times; error bars are SEM; $n = 16$).

paradox. In theory, disliking the bet on a red draw from the ambiguous deck implies that its subjective probability is lower [P_{amb}(red) < P_{risk}(red)]. The same aversion for the blue bets implies P_{amb}(blue) < P_{risk}(blue). But these inequalities, and the fact that the probabilities of red and blue must sum to 1 for each deck, imply $1 = P_{amb}$(red) + P_{amb}(blue) < P_{risk}(red) + P_{risk}(blue) = 1, a contradiction. The paradox can be resolved by allowing choices to depend both on subjective probabilities of events and on the ambiguity of those events (5–7). More generally, choices can depend on how much relevant information is missing or how ignorant people feel compared to others (8, 9).

We explored the neural differences with varying levels of uncertainty by using a combination of data from functional magnetic resonance imaging (fMRI) and behavioral data from lesion patients. This study builds on previous findings in neuroscience on reward and uncertainty. In particular, we focus on the striatum, which has been implicated in reward anticipation (10); the orbitofrontal cortex (OFC), where patients with lesions perform poorly on behavioral tasks involving uncertainty, such as the Iowa gambling task (11); and the amygdala, which responds to ambiguous facial cues and has been hypothesized as a generalized vigilance module in the brain (12–14).

The fMRI study used three experimental treatments: The Card-Deck treatment is a baseline pitting pure risk (where probabilities are known with certainty) against pure ambiguity. The Knowledge treatment uses choices about events and facts, which fall along a spectrum from risk to ambiguity. In the Informed Opponent treatment, the subject bets against another person who has seen a sample of cards from the deck. This opponent is therefore better informed about the contents of the ambiguous deck (15). This condition corresponds to a commonly posited theory of ambiguity aversion: Even when there is no informed opponent, people act as if there is (16). All three treatments have one condition where the subject is missing information (ambiguity) relative to the other condition (risk).

Subjects made 48 choices in each treatment between certain amounts of money and bets on card decks or events (17). The amounts of the certain payoff and the bet payoff varied across trials. In the Card-Deck and Informed Opponent treatments, the number and proportions of cards also varied. We estimated a general linear model (GLM) using standard regression techniques (17). Two primary regressors were used for each treatment—one for ambiguity trials and one for risky trials—beginning at the onset of the stimulus and ending at the time of decision. To find regions differentially activated by ambiguity and risk, we performed a random-effects analysis pooling all three treatments, correcting for nonsphericity (17).

Regions that were more active during the ambiguous condition relative to the risk condi-

In experiments with these choices, many would rather bet on a red draw from the risky deck than on a red draw from the ambiguous deck, and similarly for blue (3, 4). If betting preferences are determined only by probabilities and associated payoffs, this pattern is a
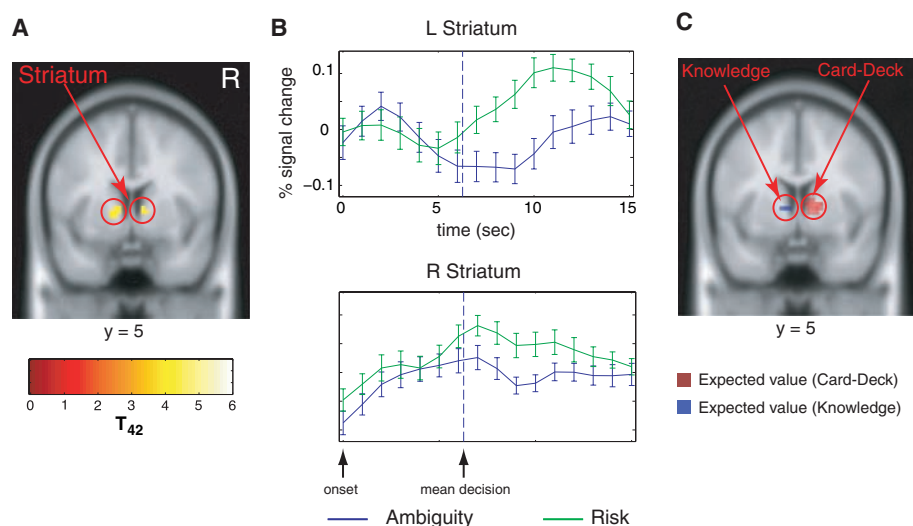
tion included the OFC and amygdala (Fig. 2A) and the dorsomedial prefrontal cortex (DMPFC) (fig. S8 and table S7). These areas have been implicated in integration of emotional and cognitive input (OFC) (*18*), reaction to emotional information (amygdala) (*19–21*), and modulation of amygdala activity (DMPFC) (*12*). Areas activated during the risk condition relative to ambiguity include the dorsal striatum (caudate nucleus) (Fig. 3A). Furthermore, the dorsal striatal activations were also correlated with the expected value of actual choices (Fig. 3C), whereas no such correlation was observed in the OFC or amygdala (tables S11 and S12). This, together with other studies implicating the dorsal striatum in reward prediction (*10, 22–24*), supports the hypothesis that ambiguity lowers the anticipated reward of decisions.

Time courses showed different patterns of activation in the ambiguity > risk and risk > ambiguity regions. Whereas the amygdala and OFC reacted rapidly at the onset of the trial (Fig. 2C), the dorsal striatum activity built more slowly (Fig. 3B) (fig. S4) and peaked significantly later (fig. S7) than those of the amygdala and OFC. This difference was present in all three experimental treatments (figs. S3 and S4) and appeared to be independent of subjects' choices (fig. S6) (*25*). The temporal difference between these ambiguity and risk regions is consistent with the presence of two interacting systems—a "vigilance"/evaluation system in the amygdala (*26*) and OFC, which responds more rapidly to the stimuli and grades uncertainty, and a reward-anticipation system in the striatum that is further downstream.

Parameters measuring ambiguity and risk aversion (γ and ρ, respectively) were estimated from a nonlinear stochastic model of the subjects' choice behavior in our tasks (*27*). Ambiguity aversion, measured by γ, was positively correlated with contrast values between ambiguity and risk (averaged over the three treatments) in the right OFC ($r = 0.55$, $P < 0.04$, two-tailed) and more weakly in the left OFC ($r = 0.37$, $P < 0.2$, two-tailed) (*17*).

To validate the fMRI results and establish that the OFC plays a necessary role in distinguishing levels of uncertainty, we conducted behavioral experiments similar to the card-deck task above, using a lesion method (*17*). Twelve neurological subjects with focal brain lesions were partitioned into two groups: those whose lesions included the most significant activation focus in the OFC revealed in our fMRI study ($n = 5$), and a comparison group (temporal lobe damage patients) whose lesions did not overlap with any of our fMRI foci ($n = 7$). The two groups had similar etiology, IQ, mathematical ability, and performance on other background tasks (table S15).

Two-dimensional confidence interval analysis (Fig. 4) showed that frontal patients are risk- and ambiguity-neutral (i.e., the hypothesis that $\gamma = \rho = 1$ cannot be rejected). This differed from the comparison group, who appeared to be risk- and ambiguity-averse. The OFC-lesioned group therefore did not distinguish between degrees of uncertainty (ambiguity and risk). This is behaviorally abnormal but is consistent, ironically, with the logic of subjective expected utility theory.

Fig. 3. Regions showing greater activation in response to risk than in response to ambiguity. Random-effects analysis of all three treatments revealed brain regions that are differentially activated in decision-making under risk. These regions include (**A**) dorsal striatum, as well as precuneus and premotor cortex (table S8) ($P \leq 0.001$, uncorrected; cluster size $k \geq 10$ voxels.) (**B**) Mean time courses for risk regions (time synched to trial onset, dashed vertical lines are mean decision times; error bars are SEM; $n = 16$). (**C**) Regions of the dorsal striatum significantly correlated with expected values of subjects' choices in risk condition of Card-Deck treatment (red) and both risk and ambiguity conditions of Knowledge treatment (blue) ($P < 0.005$, uncorrected; cluster size $k \geq 10$ voxels).
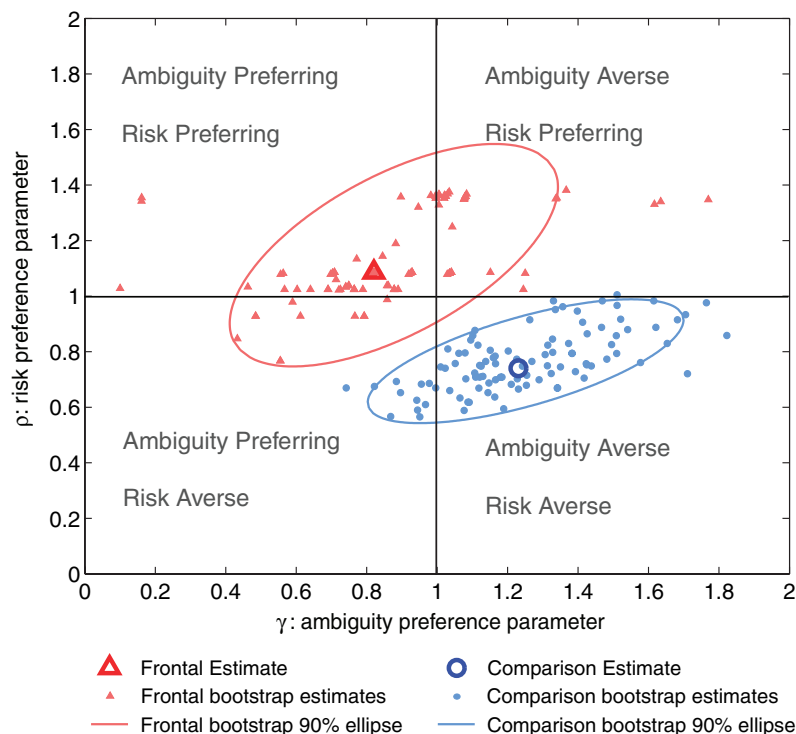
Fig. 4. Risk and ambiguity attitudes of OFC patients ($n = 5$) and lesion comparisons ($n = 7$) with associated 90% confidence intervals. The risk neutral line ($\rho = 1$) and the ambiguity neutral line ($\gamma = 1$) demarcate four quadrants as labeled. Open symbols plot maximum likelihood estimates of a group-level stochastic choice model. Frontals: ($\gamma = 0.82$, $\rho = 1.09$); lesion comparisons: ($\gamma = 1.23$, $\rho = 0.74$) [see (*17*)]. Solid symbols represent 100 bootstrapped (γ, ρ) estimates. Ellipses are two-dimensional 90% confidence intervals around the bootstrapped data. Angle of the ellipse reflects correlation between ρ and γ (0.42 for frontal, 0.31 for comparison).

Together with the fMRI results, these data suggest a neural system for evaluating general uncertainty. Both the amygdala and OFC are known to receive rapid, multimodal sensory input; both are bidirectionally connected and are known to function together in evaluating the value of stimuli (*28*); and both are likely involved in detecting salient and relevant stimuli of uncertain value. The latter function has been hypothesized especially for the amygdala (*26*, *29*). Such a function also provides a reward-related signal that can motivate behavior, by virtue of the known connections between the amygdala/OFC and the striatum (*30*). Although the circuit is assessed here in the context of a neuroeconomic experiment, we believe that it subserves general aspects of how organisms explore their environment: Under uncertainty, the brain is alerted to the fact that information is missing, that choices based on the information available therefore carry more unknown (and potentially dangerous) consequences, and that cognitive and behavioral resources must be mobilized in order to seek out additional information from the environment.

Understanding the neural basis of choice under uncertainty is important because it is a fundamental activity at every societal level, with examples as diverse as people saving for retirement, companies pricing insurance, and countries evaluating military, social, and environmental risks (*17*). The choices can vary greatly in the level of information available to the decision-maker about outcome probabilities. Standard decision theory, however, precludes agents from acting differently in the face of risk and ambiguity. Our results show that this hypothesis is wrong on both the behavioral and neural level, and suggest a unified treatment of ambiguity and risk as limiting cases of a general system evaluating uncertainty. For neuroscientists, these results introduce the important concept of varying degrees of uncertainty that is missing from previous studies of reward and decision-making. More generally, this study shows the value of combining ideas and tools from social and biological sciences (*31*, *32*).

References and Notes

1. C. Camerer, M. Weber, *J. Risk Uncert.* **5**, 325 (1992).
2. D. Ellsberg, *Q. J. Econ.* **75**, 643 (1961).
3. S. Becker, F. Brownson, *J. Polit. Econ.* **72**, 62 (1964).
4. K. MacCrimmon, *Risk and Uncertainty*, K. Borch, J. Mossin, Eds. (Macmillan, London, 1968).
5. If ambiguous probabilities are subadditive, then 1 − P_{amb}(red) − P_{amb}(blue) represents reserved belief and indexes the degree of aversion to ambiguity. Some models assume that probabilities are additive but are set-valued, and assume that the worst probability in the set determines their chances (*6*, *7*). This model and others are silent about possible neural circuitry.
6. D. Schmeidler, *Econometrica* **57**, 571 (1989).
7. I. Gilboa, D. Schmeidler, *J. Math. Econ.* **18**, 141 (1989).
8. D. Frisch, J. Baron, *J. Behav. Decision Making* **1**, 149 (1988).
9. C. Fox, A. Tversky, *Q. J. Econ.* **110**, 585 (1995).
10. W. Schultz, *Nat. Rev. Neurosci.* **1**, 199 (2000).
11. A. Bechara, D. Tranel, H. Damasio, *Brain* **123**, 2189 (2000).
12. H. Kim et al., *J. Cogn. Neurosci.* **16**, 1730 (2004).
13. H. Kim, L. H. Somerville, T. Johnstone, A. L. Alexander, P. J. Whalen, *Neuroreport* **14**, 2317 (2003).
14. E. Phelps et al., *J. Cogn. Neurosci.* **12**, 729 (2000).
15. The Informed Opponent treatment is as follows: (i) Both subjects choose a color, with the opponent having sampled the specified number of cards from the ambiguous deck; (ii) a card is chosen from the deck; and (iii) the person with the color that matches that of the card chosen wins the bet. Mismatches make nothing (*17*). The Informed Opponent hypothesis is that bets on ambiguous card decks and low-knowledge events, although normatively different from bets against the informed opponent, are generated by similar neural circuitry. Similarity of time courses in the amygdala, OFC, and striatum across all three treatments (figs. S3 and S4) is consistent with this hypothesis.
16. A. Kühberger, J. Perner, *J. Behav. Decision Making* **16**, 181 (2003).
17. See supporting data on *Science* Online.
18. H. Critchley, C. Mathias, R. Dolan, *Neuron* **29**, 537 (2001).
19. A. Bechara, H. Damasio, A. Damasio, *Ann. N.Y. Acad. Sci.* **985**, 356 (2003).
20. R. Adolphs, *Curr. Opin. Neurobiol.* **12**, 169 (2002).
21. H. Critchley, R. Elliot, C. Mathias, R. Dolan, *J. Neurosci.* **20**, 3033 (2000).
22. J. O'Doherty et al., *Science* **304**, 452 (2004).
23. B. Knutson, C. Adams, G. Fong, D. Hommer, *J. Neurosci.* **21**, RC159 (2001).
24. One earlier positron emission tomography study (*33*) also found differential activation in the caudate during risk relative to ambiguity (www.econ.umn.edu/~arust/C-CAll.pdf, p6).
25. The areas that are differentially activated by the choice that subjects make (gamble or certain payoff) include the caudate head and the insula (table S9), which are also not significantly interacting with ambiguity/risk.
26. P. J. Whalen, *Curr. Direct. Psychol. Sci.* **7**, 177 (1998).
27. Aversion to risk is measured by the concavity of the subjective utility function for money, $u(x) = x^\rho$. Lower ρ corresponds to more risk aversion. Aversion to ambiguity (controlling for risk aversion) is measured by the degree to which probabilities P are underweighted when they are ambiguous, $w(P) = P^\gamma$. Higher γ corresponds to more ambiguity aversion. Best fitting values of ρ and γ are estimated via maximum likelihood (*17*).
28. D. Gaffan, E. A. Murray, M. Fabre-Thorpe, *Eur. J. Neurosci.* **5**, 968 (1993).
29. R. B. Adams Jr., H. L. Gordon, A. A. Baird, N. Ambady, R. E. Kleck, *Science* **300**, 1536 (2003).
30. D. Amaral, J. Price, A. Pitkanen, S. Carmichael, in *The Amygdala: Neurobiological Aspects of Emotion, Memory, and Mental Dysfunction*, J. P. Aggleton, Ed. (Wiley, New York, 1992), pp. 1–66.
31. P. Glimcher, A. Rustichini, *Science* **306**, 447 (2004).
32. S. M. McClure, D. Laibson, G. Loewenstein, J. D. Cohen, *Science* **306**, 503 (2004).
33. A. Rustichini, J. Dickhaut, P. Ghiradato, K. Smith, J. Pardo, *Games Econ. Behav.* **52**, 257 (2005).
34. We thank K. Scheer and M. Koenigs for data collection, and P. Bossaerts and S. Quartz for valuable input in the planning stages of this work. Supported by NSF grant SES 0433010 (C.C. and R.A.), the MacArthur Foundation Preferences Network (C.C.), Caltech grant CFC.PROVOST-3-GRANT (C.C.), NIH grants R01 MH067681 (R.A.) and P01 NS19632 (D.T.), and the David and Lucile Packard Foundation.

A Conserved Checkpoint Monitors Meiotic Chromosome Synapsis in *Caenorhabditis elegans*

Needhi Bhalla[1,2] and Abby F. Dernburg[1,2]*

We report the discovery of a checkpoint that monitors synapsis between homologous chromosomes to ensure accurate meiotic segregation. Oocytes containing unsynapsed chromosomes selectively undergo apoptosis even if a germline DNA damage checkpoint is inactivated. This culling mechanism is specifically activated by unsynapsed pairing centers, *cis*-acting chromosome sites that are also required to promote synapsis in *Caenorhabditis elegans*. Apoptosis due to synaptic failure also requires the *C. elegans* homolog of *PCH2*, a budding yeast pachytene checkpoint gene, which suggests that this surveillance mechanism is widely conserved.

Meiosis requires two successive cell divisions: one in which homologous chromosomes separate and a second that partitions sister chromatids. Accurate segregation depends on the establishment of physical linkages (chiasmata) between homologous chromosomes during meiotic prophase. Chromosome pairing, the polymerization of the synaptonemal complex between paired homologs (synapsis), and crossover recombination are all required to generate chiasmata,

which enable proper chromosome alignment on the meiotic spindle.

Defects in these early meiotic events can lead to cell cycle arrest or apoptosis, indicating that the events are monitored by checkpoints. In budding yeast, a "pachytene checkpoint" responds to defects in homolog synapsis and/or recombination [reviewed in (*1*)]. Mammalian meiosis may have two distinct checkpoints, one that responds to synaptic failure and one that responds to DNA damage (*2–4*). Because synapsis and recombination are obligately coupled in both *Saccharomyces cerevisiae* (*5*) and mice (*3*, *6*), it has been ambiguous whether these checkpoints are triggered by recombination defects or asynapsis. Here, we have exploited the knowledge that synapsis can be complete-

[1]Life Sciences Division, Lawrence Berkeley National Laboratory, [2]Department of Molecular and Cell Biology, University of California, Berkeley, Berkeley, CA 94720, USA.

*To whom correspondence should be addressed. E-mail: afdernburg@lbl.gov

Supporting Online Material for

Neural Systems Responding to Degrees of Uncertainty in Human Decision-Making

Ming Hsu, Meghana Bhatt, Ralph Adolphs, Daniel Trane, Colin F. Camerer*

*To whom correspondence should be addressed. E-mail: camerer@hss.caltech.edu

This PDF file includes:

Supplementary Methods

1 Methods

Subjects: Sixteen Caltech undergraduate and graduate students were recruited from the Caltech Social Science Experimental Laboratory database to participate in the study (13 males, 3 females). The mean (std. dev.) age was 23.5 years (6.2). Informed consent was obtained using a consent form approved by the Internal Review Board at Caltech. Subjects read written instructions before entering the scanner (included at the end of the supplements). After reading the instructions they completed a quiz to ensure comprehension of how their decisions affected their performance and earnings. They knew that at the end of the experiment, one trial from each of the three treatments would be chosen at random, and their choice on that trial would determine their pay. Their earnings were the total from the three randomly-chosen choices, plus $5 fee for participating.

Behavioral task: Stimuli were presented through MRI compatible goggles (Resonance Technology). Choices were made using an MRI-compatible button box. For each choice, three options were given. Two of the options were bets on either side of a binary choice gamble that carried some uncertainty of paying either a positive sum or zero. The third option was the sure payoff that paid a certain positive amount of money. Subjects were allowed as much time as they desired in making their choice. Responses were made by pressing the button corresponding to the location of the options (left-middle-right) on the screen.

The gambles were not played after each trial because then the degree of ambiguity would change over time as subjects learned from feedback about the event probabilities.

Card-deck treatment: In the Card-Deck treatment, subjects take the sure payoff, or bet on either red or black card. The cards are blue in the presentation because the background was black, but conventional red and black playing cards were used to determine the actual payoff after the subject came out of the scanner. Subjects knew blue and black were equivalent. Full list of stimuli are presented in Table S1.

Knowledge treatment: In the Knowledge treatment, subjects could take the sure payoff, or bet on whether the answer was Yes or No to the statement presented. Full list of stimuli are presented in Table S2.

Informed Opponents treatment: In the Informed opponents treatment, subjects either take the sure payoff, or bet that a red or black card would be drawn. If they choose the bet, they play against an opponent that will sample from the an ambiguous deck the number of cards indicated on the screen.

If the colors of the cards chosen by the subject and his/her opponent match, the bet does not take place and both earn the sure payoff instead. If the colors mismatch, the bet takes place, and the subject whose card matches the color of the card randomly chosen from the deck, wins the amount indicated on the screen, with the other subject earning 0.

Note that because the opponent chooses a color *after* seeing a sample of cards, the opponent always has more information than the subject, in the "low-information" condition where one or more cards are drawn. For example, if the scanned subject chooses to bet on red, then her bet only counts if the informed opponent bet black (because she saw that more of the drawn cards were black than red. Thus, the scanned subject is always betting on the *opposite* of the color which was most common in the 3-card sample or, equivalently, the scanned subject is always betting on the less likely color (this is called "adverse selection" in economics). The scanned subjects *should* be averse to betting against the informed opponent. In the 0-draw case both players have the same information so there is no rational reason to dislike betting. Full list of stimuli are presented in Table S3.

Table S4 shows mean response times across conditions and treatments. Because response times are skewed and bounded away from zero, standard deviations are large and misleading about distributional variance. Figure S1 therefore displays boxplots of the log response times of choices by type of choice, condition, and treatment. These boxplots show that there are no significant differences in the central tendency of response times between any of these variables.

The proportion of choices of the certain payoff for each question is presented in Tables S1-3. Summary of the proportion of choices made by subjects are presented in Figure S2 and Table S5. Roughly speaking, a greater number of certain choice indicates greater ambiguity/risk aversion. A more rigorous demonstration of ambiguity/risk aversion is presented in Section 1.1.

The fMRI analysis used 16 subjects. All 16 completed the Card-Deck and Knowledge treatments, and 13 completed the Informed Opponent Treatment (which always came last). The order of treatments was fixed across trials. Order was not counterbalanced because the deck in the Informed Opponents treatment is the same as the ambiguous deck in the Card-Deck treatment. Presenting the Informed Opponents Treatment before the Card-Deck treatment might introduce a "hierarchy" of uncertainty that we did not wish to introduce to the experiment.

Each treatment is composed of 48 trials in each of the three treatments, 24 ambiguous and 24 risky. Trials are presented in blocks consisted of four ambiguous or four risky trials in order, alternated with blocks of the opposite type. After each decision, the stimulus remained onscreen for 2 seconds, followed by a fixation cross for 4-8 secs (randomized) before the next stimulus presentation.

1.1 Behavioral data analysis

A parametric analysis to estimate risk and ambiguity was conducted via a nonlinear stochastic choice model.

Subject's utility functions for money are assumed to follow a power function $u(x, \rho) = x^\rho$, which is conveniently characterized by one parameter and widely used in empirical estimation of this sort. Subjects are assumed to weight probabilities according to the function $\pi(p, \gamma) = p^\gamma$.

The ρ parameter is interpreted as the risk aversion coefficient, i.e., the curvature of the utility function. The γ parameter is interpreted as the ambiguity aversion coefficient, i.e., how much do people over(under)-weight probabilities because they are not confident in their judgments. If subjects over-weight ambiguous probabilities ($\gamma < 1$), we characterize them as ambiguity-preferring. If they under-weight ambiguous probabilities ($\gamma > 1$), we characterize them as ambiguity-averse.

If subjects weight probabilities linearly ($\gamma = 1$), we characterize them as ambiguity-neutral. We assume subjects combine these weighted-probabilities and utilities linearly, so that their weighted subjective expected utility is $U(p, x, \gamma, \rho) = \pi(p, \gamma)u(x, \rho)$.

The tasks are binary choices in which subjects either choose a gamble to win x (with probability p) or 0, or a certain payoff c. For the risky deck, the ratios of the cards are the probabilities. For the ambiguous decks and all knowledge questions, we assumed $p = 1/2$. If subjective p is different than $1/2$ (e.g., because a subject happens to know a lot about fall temperatures in New York), then subjective probabilities are not held constant across the knowledge trials. This possibility biases our analysis against finding common regions of activation across treatments, so would imply that the results described in the text are conservative about the true extent and commonality of ambiguity and risk-specific regions. We constrain $\gamma = 1$ in all risk conditions and estimate γ from behavioral data in the ambiguity conditions (*S1*).

The probability that the subject chooses the gamble rather than the sure amount c is given by the logit or softmax formula, $P(p, x, c, \gamma, \rho) = 1/(1 + exp\{-\lambda(U(p, x, \gamma, \rho) - u(c, \rho))\})$, where λ is the sensitivity of choice probability to the utility difference (the degree of inflection), or the amount of "randomness" in the subject's choices ($\lambda = 0$ means choices are random; as λ increases the function is more steeply inflected at zero).

Denote the choice of the subject in trial i to be y_i, where $y_i = 1$ if subject chooses the gamble, and 0 if the certain payoff.

We fit the data using maximum likelihood, with the log likelihood function

$$\sum_{i=1}^{48} y_i \log(P(p_i, x_i, c_i, \gamma, \rho, \lambda)) + (1 - y_i) \log(1 - P(p_i, x_i, c_i, \gamma, \rho, \lambda)).$$

Because this is a nonlinear optimization problem, numerical methods must be used. We used the Nelder-Mead simplex algorithm implemented in Mathematica v5.1(*S3*), with 10 random starting positions. The iteration with the highest likelihood value was chosen. Table S6 shows the estimates from the fMRI subjects.

2 FMRI acquisition

Imaging was performed using a 3 Tesla Siemens Trio scanner at the Broad Imaging Center at Caltech. A set of high-resolution (0.5mm x 0.5mm x 1.0mm) T1-weighted anatomical images was first acquired to enable localization of functional images. Whole-brain functional images were acquired in 32-34 axial slices (64 x 64 voxels; in plane resolution 3 mm x 3 mm x 3.5 mm slices) at a TR of 2000 msec, TE of 30 msec.

The scan sequences were axial slices approximately parallel to the AC-PC axis. Scan sequences were not optimized for the OFC, therefore susceptibility artifacts affected adversely the image quality of the medial OFC. The lateral OFC activation found in the experiment, however, is sufficiently distant to the signal dropout regions as to not be adversely affected.

Prior to analysis, the images were corrected for slice time artifacts, realigned, coregistered to the subject's T1 image, normalized to Montreal Neurological Institute coordinates (resampled 4mm x 4mm x 4mm), and smoothed with an 8mm full-width-at-half-maximum Gaussian kernel using SPM2 (*S4*). At the start of each functional scanning run, the screen remained black for 4s to allow time for magnetization to reach steady state. The associated first two images were discarded from the analysis. Thirteen out of 16 subjects completed all tasks within three 15-minute scanning runs. However, the duration of the experiment was variable because choices were self-paced. Three subjects did not have time to complete the Informed Opponent treatment.

3 FMRI Analysis

The general linear model (GLM) and random effects analyses presented in Figures 1 and 2 were performed using SPM2 (*S4*). For each treatment, two regressors were included to identify the risk and ambiguity regions. Each regressor modeled the entire duration of the trial. A third regressor was defined at the time of decision, which controlled for motor responses.

Each regressor was generated by convolving a canonical hemodynamic response with a dummy variable that equaled 1 during the ambiguity (risk) trial (from onset to decision), and 0 for all other points.

The regressors were anchored to stimulus presentation based on the hypothesis that the reaction to uncertainty would occur between stimulus onset and the time of decision, rather than afterwards as a result of the decision (since there is no feedback after each trial). We did not include onset *and* decision epochs for both ambiguity and risk in the model because the parameters then become unidentified due to multicollinearity.

Each subject thus generated the set of contrasts ambiguity>risk and risk> ambiguity for each treatment, for a total of 6 contrasts. A one-way ANOVA was conducted in SPM2 to find the areas of joint significance, correcting for non-sphericity due to repeated measures. That is, we pooled all of the ambiguity>risk contrasts, and conducted a t-test on whether the average response in the three treatments were significantly greater than 0. The same procedure was used for the risk>ambiguity contrast.

Results are reported for brain areas that are significant at $p < 0.001$ uncorrected and cluster size $k \geq 10$. An exclusive mask was used to exclude voxels that are significantly different between the three sessions ($p < 0.01$). The rationale for this exclusion is that voxels/regions significantly different across the three treatments suggests that they do not perform the same function (*S5*).

The impact of the exclusive mask had negligible qualitative effect on the data. The only notable effect was in reducing the corrected p-value through reducing the search volume of the brain (because of exclusion of voxels). Uncorrected p-values, of course, were unaffected.

Table S7 presents fMRI results for the ambiguity>risk model. Table S8 presents results for

the risk>ambiguity model. Figures S3-S4 show the HRF's of percentage signal change in these two contrasts for each of the three tasks separately, to show the robustness of the effect across tasks.

3.1 Decision-epoch synched model

A model with regressors anchored to the decision epoch was also estimated for all subjects. This provides a robustness check on our assumption that the hemodynamic responses in our regions were synced to the onset of the stimulus, rather than that of the decision. Results from this model showed similar activation in the dorsal striatum for the risk $>$ ambiguity contrast, but did not show differences in the amygdala or lateral OFC (Fig. S5). It is clear from the hemodynamic responses in Figure 2B and 3B why this is so. The activations in the OFC and amygdala occur at the beginning of the trial, and peaks before the decision epoch. The striatal activity occurs somewhere between the onset and the decision, which allows it to be captured by the decision-synched model.

3.2 Choice-dependent regions

Tables S9-S10 present all regions differentially activated under gamble and certain payoff choices ($p < 0.001$ uncorrected, $k \geq 10$ voxels). In addition to contralateral visual and motor activations, corresponding to the visual inputs and motor responses required to make the choices, there were significant bilateral insula and left ventral striatum activation in the gamble>certain contrast. This is consistent with previous findings of insular activity in decision making under risk ($S7$).

These regions, however, did not exhibit significant interaction with the ambiguity/risk distinction. Together with the fact that the risk/ambiguity regions did not exhibit significant differences across choices, this suggests that the risk/ambiguity regions are indeed responding to the ambiguity/risk trial dimension (Fig. S6) rather than to gamble/certain choices.

3.3 Expected reward regions

To identify regions that were sensitive to expected dollar value of rewards, conditional on the subject's choice, we used a model where the event of interest was synched to the decision epoch.

Two different main regressors were used for the ambiguity and risk conditions, respectively. Each regressor was associated with an interaction term defined by the expected dollar value of the actual choice (either the gamble or the certain payoff). Notice that sometimes the choice was the certain payoff and sometimes it was the gamble, so this interaction should detect regions that are sensitive to expected value of the actual choice, regardless of whether it was a certain or uncertain amount.

Results from this analysis are presented in Table S11-S12. In the Card-Deck treatment, activity in the right dorsal striatum was correlated with the expected reward in the risk condition. Activity in left dorsal striatum was correlated with the expected reward in both conditions of the Knowledge treatment. More importantly, the dorsal striatum regions found in this analysis also overlapped with the risk> ambiguity regions found in the main analysis. No consistent activations were found in the Informed Opponents treatment (*S8*).

It is interesting to note that the lateralization corresponds to the semantic/mathematical lateralization. It is less clear, however, how much of this dissociation is due to the ambiguity/risk distinction, or the lack of information about the expected reward in the ambiguity condition. Further research would be needed to establish this relationship.

3.4 Cross-Correlation

Table S13 presents the cross-correlation of contrast values in our regions of interest. The OFC and amygdala contrast values are from ambiguity-risk contrast and striatum the opposite so a positive table entry between those areas is a negative correlation. These correlations show a modest link between amygdala and OFC, and a substantial (negative) correlation between striatum and OFC (again, the correlations shown are negative but since contrasts are opposite, should be interpreted as positive). This is consistent with the hypothesis that OFC is judging

gradations of uncertainty and triggering differential striatal responses.

4   Lesion Data

4.1   Lesion Patient Information

Twelve neurological patients with single, focal, stable, chronic lesions of the brain were chosen from the Iowa Cognitive Neuroscience Patient Registry such that they were similar in terms of the etiology of their lesions (surgical resection), and similar on background neuropsychological measures. We partitioned the patients on the basis of whether or not their lesion overlapped with the largest and most significant frontal activation focus we found in the fMRI study (Right lateral OFC, cf. Fig. 2 and Table S7), or whether their lesion did not overlap with any significantly activated region. These two groups, designated "frontal" and "comparison" consisted, respectively, of 5 (3 males, 2 females) and 7 patients (4 females, 3 males). The frontal group had lesions in bilateral OFC and frontal pole (1 patient), right OFC and right insula (1 patient), right OFC and frontal pole (1 patient) or only right OFC (2 patients) resulting from neurosurgical resection of brain tumors (frontal meningeoma resection). The comparison group had lesions in left (3 patients) or right (3 patients) anterolateral temporal cortex, or in left posterior temporal cortex (1 patient) resulting from neurosurgical resection for the treatment of epilepsy. There were no significant differences between these groups in the overall size of the lesion.

Summary of behavioral data for these patients are shown in Table S14. All subjects had IQs in the normal range, had normal memory performance and arithmetic abilities, and were not aphasic, depressed, or perseverative (Table S15). Frontal-damage patients were not significantly different than the temporal-damage comparison group except on the PIQ test where frontal patients scored higher than the temporal comparison group ($p < .05$).

4.2   Estimation Procedure

The lesion patient choices were part of a larger battery of decision and game tasks.

In the ambiguity condition, patients were shown an actual card deck with 20 cards, in some mixture of red and black they could not see. They were given a series of choices between certain amounts of points (15, 60, 30, 40, 25 in that order) and bets on the color of their choice from the card deck for 100 points.

To illustrate, an ambiguity- and risk-neutral person would choose from the deck rather than take the certain amounts 15, 30, 40, or 25, but would take the certain 60 rather than choose from the deck. In the risky condition they were shown a deck with exactly 10 red and 10 black cards whose colors they could see. They made choices between a bet on the color of their choice from the deck for 100 points, or certain amounts of 30, 60, 15, 40, and 25 (in that order).

There are three small differences in this task and the Card-Deck treatment in the fMRI experiment: (1) There were fewer choices in the lesion experiment, due to time constraints in conducting experiments with lesion patients and the need for multiple trials to extract fMRI signal; (2) there was wider range of certain point amounts in the lesion task (in case patients were extremely risk- and ambiguity-averse or -preferring); and (3) due to human subjects restrictions, the lesion task choices were not conducted for actual monetary payments. Feature (1) means we could estimate ρ and γ for each individual in the fMRI study but were forced to pool data within each patient group for the OFC-comparison analysis. Note that the methodological differences (1-3) between the fMRI and lesion tasks do not matter for the most important finding from the lesion task, which is the significant difference between OFCs and the comparison group (Fig. 4).

Data from all subjects were pooled within each group (summary of aggregate data are presented in Table S14). This yielded 25 choices (from 5 subjects) for the frontal group, and 35 choices (from 7 subjects) for the comparison group. The maximum likelihood estimation procedures are identical to those discussed above. To derive confidence intervals, a bootstrap procedure was used with 100 runs: For k-subject groups, a pseudosample consisted of k draws of different subjects *with replacement* from the sample. The estimation procedure was than applied to that pseudosample. One hundred pseudo-samples were drawn for each group (closed dots in Fig. 4).

4.3 Estimates

The estimates for lesion patients using the data were $(\gamma = 0.82, \rho = 1.09, \lambda = 0.10)$ for frontal patients, and $(\gamma = 1.23, \rho = 0.74, \lambda = 0.27)$ for the comparison group .

Across the 100 pseudo-samples, the bootstrap estimates yielded estimated means (standard deviations) of $\gamma = 0.88(0.28), \rho = 1.15(0.20), \lambda = 0.48(1.29)$ for the frontal patients, and $\gamma = 1.25(0.22), \rho = 0.77(0.11), \lambda = 0.28(0.16)$ for the lesion patients.

The only noticeable difference in the pooled estimates, and the central tendencies of the bootstrapped estimates, is the lower λ for frontals (.10) in the group procedure versus the bootstrap mean (.48). This reflects the fact that one subject behaved differently than the others and more randomly across certain-amount x values. Fitting group data including this subject requires estimation of a relatively low λ. However, in bootstrap runs this outlying subject was often not selected into the pseudosample, and in those pseudosamples more inflected responses to x deliver higher λ. The crucial parameter, the ambiguous probability discount γ, is quite close in the two types of estimation however, and is close to the ambiguity-neutral value of 1.

5 Related Literature in Social Science

In the paper we refer to several areas of social science that incorporate ambiguity aversion. For economics and politics see ($S9$); macroeconomic policy-making ($S10$); wage-setting and contracting ($S11, S12$); strategic thinking ($S13, S14$); voting ($S15$); and financial investment ($S16, S17$). Because the literature is large, we focus next only on two practical examples that clearly illustrate the nature of how ambiguity-aversion might influence practice (in law) and its potential economic importance (in finance).

Scottish law has a "not proven" verdict, along with "guilty" and "not guilty" verdicts. According to Peter Duff ($S18$), "the difference is that the verdict of 'not guilty' is thought to mean that the accused definitely did not commit the crime, that is, it is a positive declaration of innocence, whereas the verdict of 'not proven' is thought to imply solely that the accused's guilt

has not been conclusively demonstrated" (p. 193). The "not proven" and "not guity" verdicts have the same legal implications, because both prohibit retrial even in the face of new evidence. Not proven verdicts are returned in about a third of jury trials, typically when the jury thinks the defendant is actually guilty but cannot legally convict because of a lack of corroborating evidence required by Scottish law (e.g., in sexual assault where only the victim is a witness to the crime). The Scottish "not proven" verdict expresses the two dimensions of evidence noted by Keynes–when the "weight of the evidence" is light, a verdict of "not proven", and the traditional guilty and not guilty verdicts reflect the implications of weighty evidence.

One practical economic consequence of ambiguity-aversion is home bias—the tendency for investors in most countries to invest heavily in stocks from their home country and very little in stocks from foreign countries. The reluctance to hold foreign stocks amounts to a sacrifice in annual percentage return of 1-2% per year ($S19$) according to one estimate. Assuming an average unbiased return of 7% ($S20$), a person with home bias who invests a lump sum at age 25 will end up with only half as much money at age 65 as an investor who is unbiased

Home bias is large and pervasive: In 1989 American, Japanese, and British investors held 94%, 98%, and 82% of their investments in home-country stocks ($S19$) even though the latter two markets account for only a modest fraction of the world portfolio. Home bias also exists at many levels: Portfolio managers prefer to invest in companies with headquarters nearby, individuals preferred their own regional "baby Bell" companies after the breakup of AT&T, workers invest too heavily in the stock of the companies they work for, and investors in many countries prefer to invest in nearby companies or those whose managers speak the same language that they do ($S21$).

In most cases, the stock returns from investing in familiar stocks are not higher than unfamiliar ones, so the home bias is consistent with a pure distaste for betting on ambiguous foreign or faraway assets (as in our Knowledge treatment).

Supporting Figures and Legends
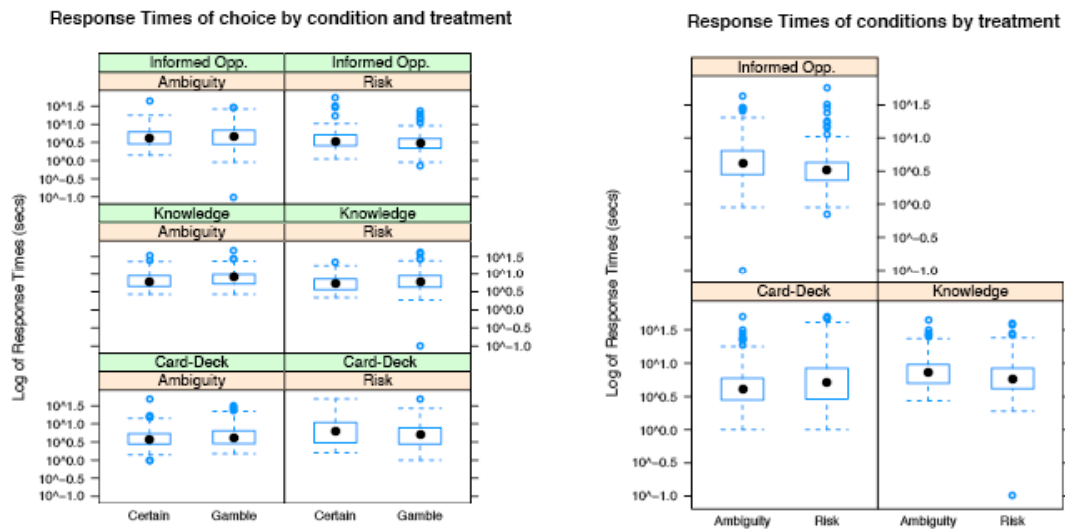
Figure S1: Boxplots of log response times (secs) of choice by condition and treatment. Response times are logged due to skewness of the distribution. Boxplots show that there are no significant differences between choices and between conditions across the treatments.
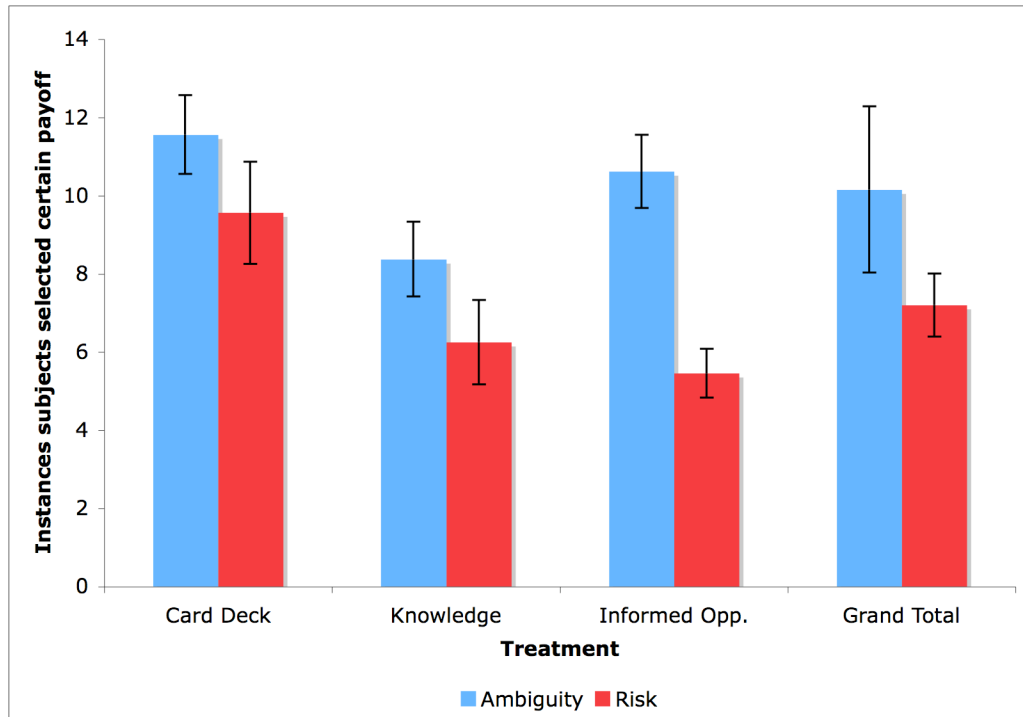
Figure S2: Choices of subjects across treatment and condition. Average of number and standard error bars of certain payoff choice by subjects across condition and treatment (out of 24 total choices per condition per treatment). A higher frequency of choosing the certain payoff in the ambiguity treatment (compared to the frequency in the risk treatment) is an indicator of ambiguity aversion.
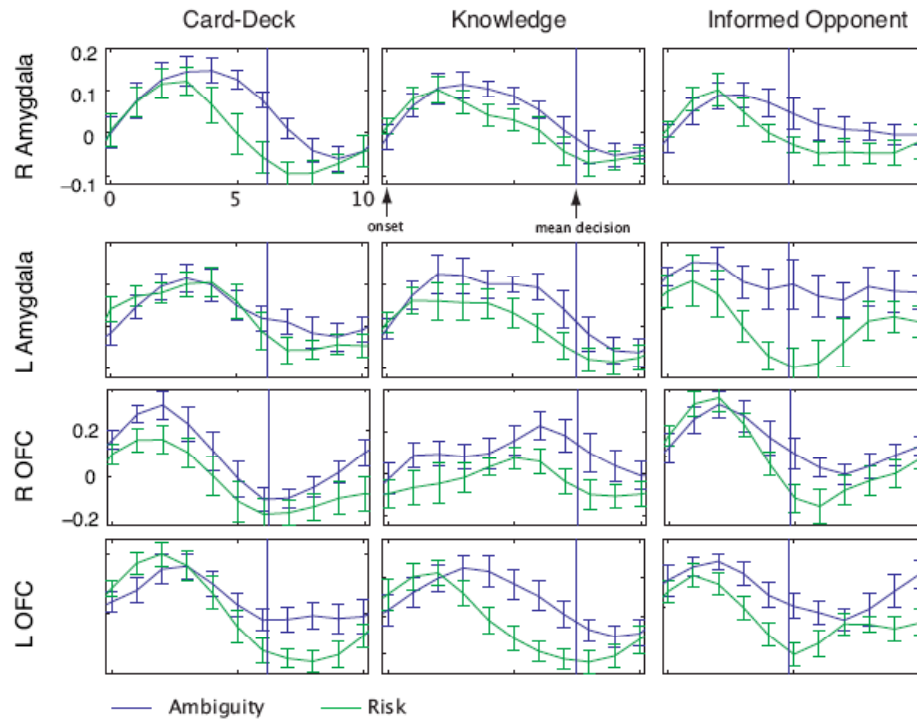
Figure S3: Treatment specific HRFs, Ambiguity > Risk. Time courses of percentage signal change in brain regions that are differentially activated in decision making under ambiguity in Card-Deck, Knowledge, and Informed Opponent conditions. Note that the effect ambiguity > risk is observed in each of the areas. Furthermore, the qualitative aspects of the activation and differences between ambiguity and risk are preserved between the pooled HRFs (Fig. 2b) and the above HRFs. Axes are the same as in the text Figures.
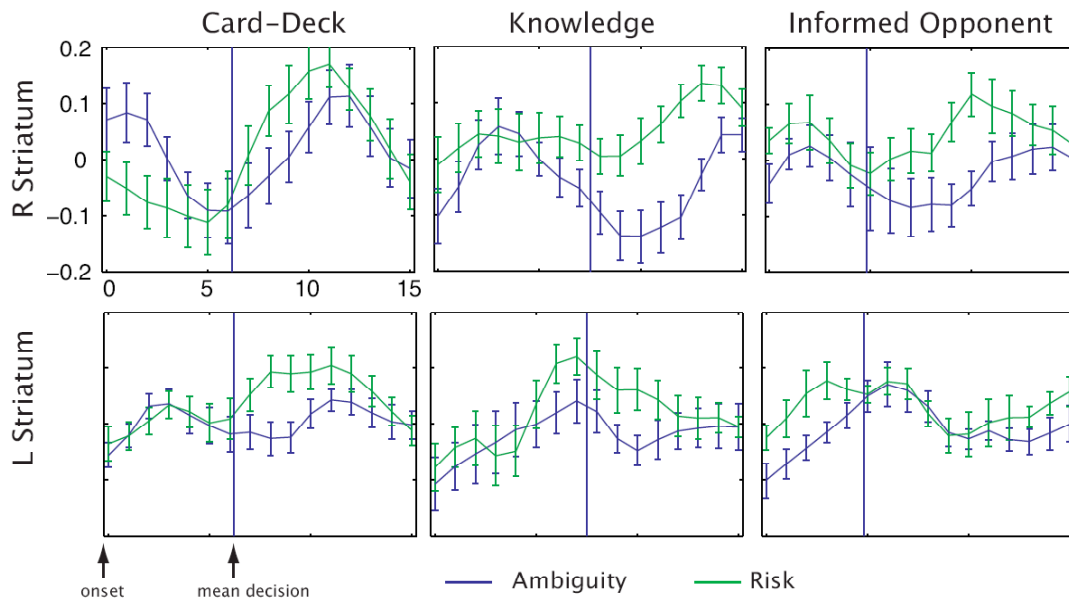
Figure S4: Treatment specific HRFs, Risk > Ambiguity. Time courses of percentage signal change in brain regions that are differentially activated in decision making under risk in Card-Deck, Knowledge, and Informed Opponent conditions. Note that the effect risk > ambiguity is observed in each of the areas. Furthermore, that the qualitative aspects of the activation and differences between ambiguity and risk are preserved between the pooled HRFs (Fig. 3b) and the above HRFs. Axes are the same as in the text Figures.
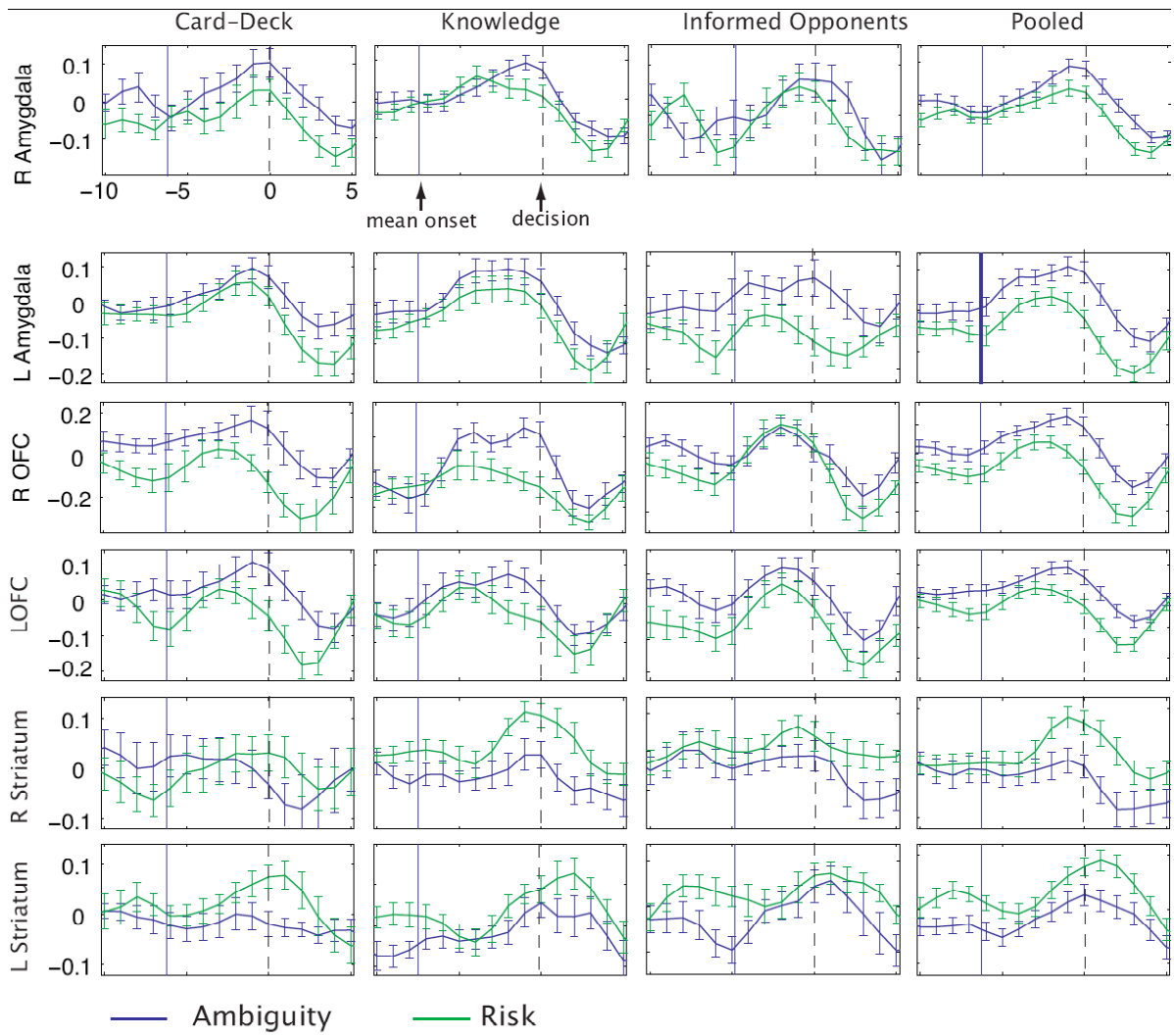
Figure S5: Decision-synched HRFs. Hemodynamic responses of regions of interest synched at decision epoch at t = 0 (dotted gray line), blue vertical line indicates mean trial onset.
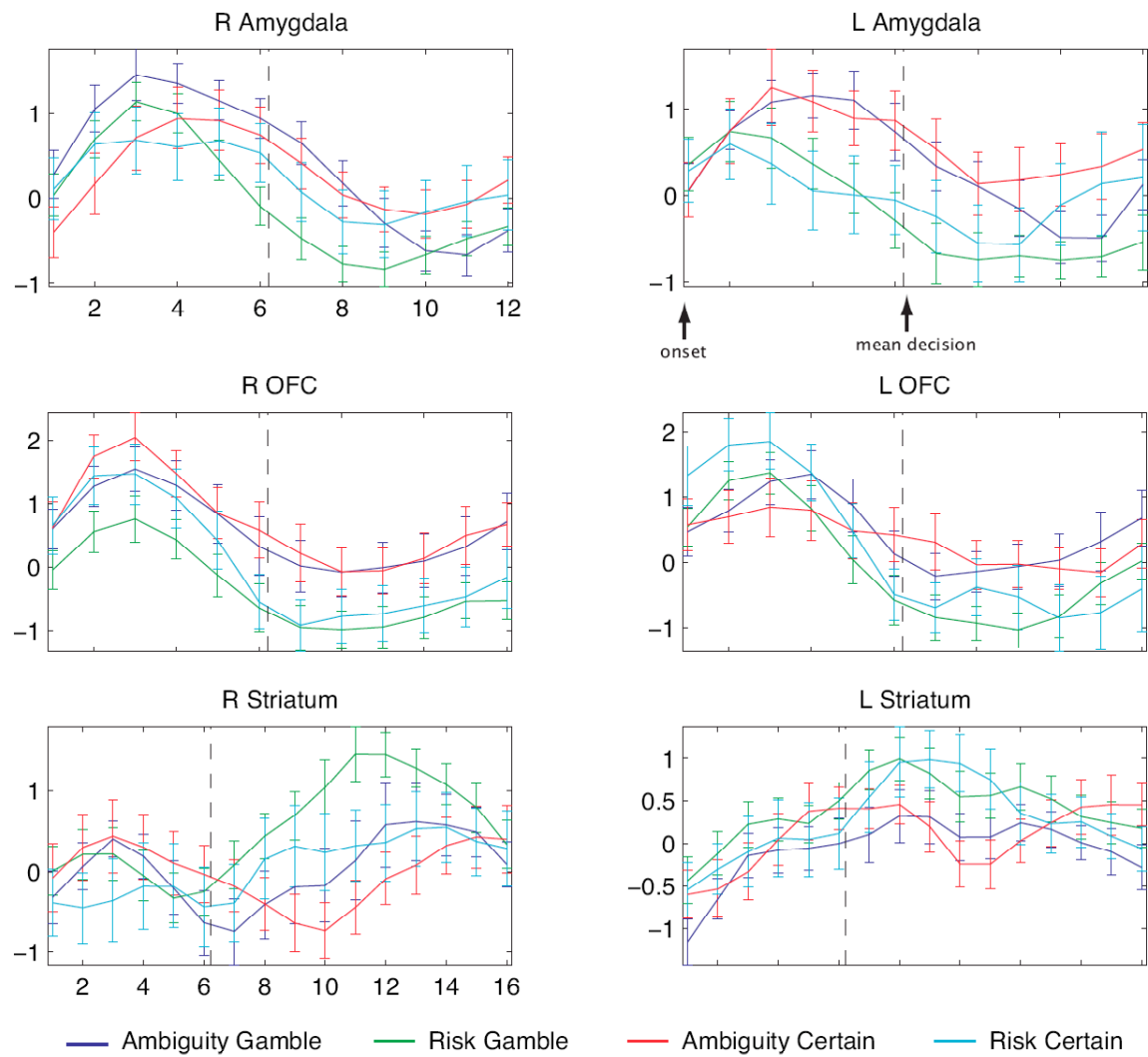
Figure S6: Pooled HRFs separated by condition (ambiguity versus risk) and actual choice (gamble versus certain). Note that no consistent differential activation can be observed between choices (gamble vs. certain).
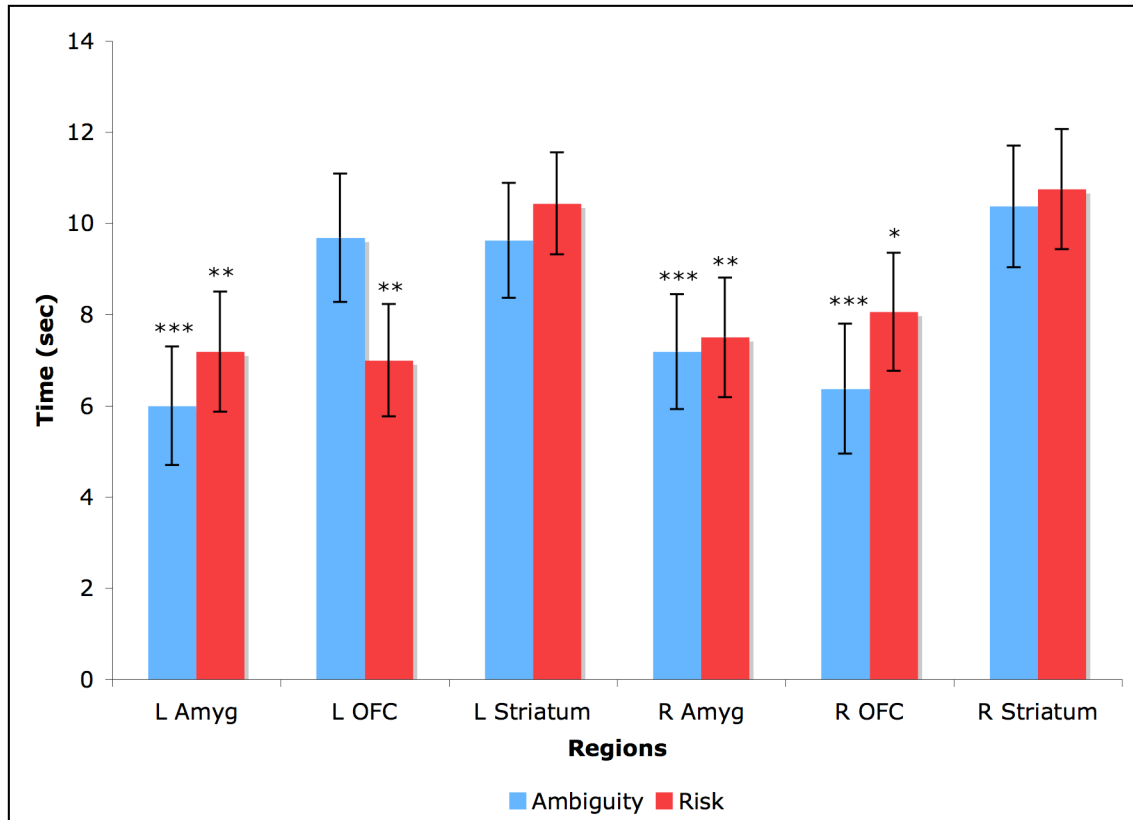
Figure S7: Mean time to peak hemodynamic response. Peaks are defined as the mean time (in seconds, measured from trial onset) to the maximum BOLD response observed, across subjects and conditions. Time window is defined as in Fig. 2 and Fig. 3 (16 secs). Note that the peaks for the left and right striatum occur significantly later than those of the amygdala and OFC, with the exception of the L OFC in the ambiguity condition. Stars denote the significance level of t-tests on whether the time to peak for the amygdala and OFC regions occur significantly later than those of the striatal regions of the same laterality and condition (all tests 2-tailed, $p < 0.1$: *, $p < 0.05$: **, $p < 0.01$: ***).
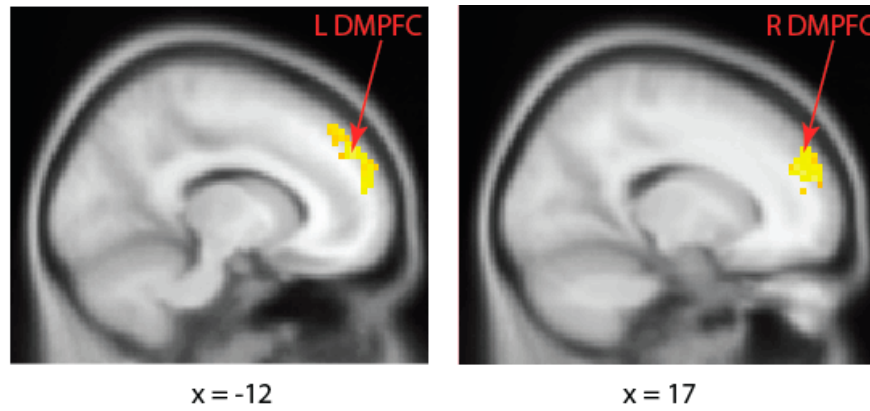
Figure S8: Dorsomedial prefrontal cortex (DMPFC) activation under ambiguity relative to risk (at $p < 0.001$, uncorrected, cluster $k > 10$ voxels).

Table S1: Parameters and Data for Card-Deck Treatment. "# Total Cards" is the number of cards in the deck. "# Blue Cards" and "# Red Cards" are the numbers of each color card in the risky deck (total number of cards is the sum of the numbers of blue and red cards). "Gamble" and "Certain" are dollar payoffs for the gamble and the certain payoff, respectively. "% Certain Choice" is the percentage of fMRI subjects who chose the certain payoff rather than the gamble in each row.

Condition	# Total Cards	Gamble	Certain	% Certain Choice
Ambiguous	15	24	11	68.75
Ambiguous	7	28	16	43.75
Ambiguous	30	27	12	37.50
Ambiguous	20	17	6	25.00
Ambiguous	40	18	9	68.75
Ambiguous	7	28	15	62.50
Ambiguous	38	23	8	31.25
Ambiguous	25	26	8	37.50
Ambiguous	15	26	15	81.25
Ambiguous	6	24	9	25.00
Ambiguous	25	17	9	50.00
Ambiguous	2	22	7	6.25
Ambiguous	15	28	15	62.50
Ambiguous	35	28	15	56.25
Ambiguous	20	27	8	31.25
Ambiguous	34	20	11	81.25
Ambiguous	10	29	17	73.33
Ambiguous	4	22	9	20.00
Ambiguous	30	22	12	73.33
Ambiguous	1	28	14	60.00
Ambiguous	40	25	10	46.67
Ambiguous	15	23	9	20.00
Ambiguous	19	30	17	60.00
Ambiguous	9	28	10	6.67

Condition	# Blue Cards	# Red Cards	Gamble	Certain	% Certain Choice
Risk	10	15	16	7	6.25
Risk	5	10	23	13	0.00
Risk	20	10	23	13	25.00
Risk	6	10	27	16	68.75
Risk	2	10	22	17	25.00
Risk	1	5	30	20	37.50
Risk	15	10	17	11	75.00
Risk	10	20	25	12	31.25
Risk	20	2	18	14	50.00

Risk	1	5	23	20	62.50
Risk	8	15	16	10	56.25
Risk	1	3	30	21	43.75
Risk	5	10	26	16	50.00
Risk	2	5	19	15	100.00
Risk	1	3	17	13	50.00
Risk	10	5	17	11	25.00
Risk	8	10	29	14	33.33
Risk	1	5	26	17	40.00
Risk	10	5	17	11	33.33
Risk	15	20	23	11	40.00
Risk	20	2	23	18	33.33
Risk	1	5	21	14	26.67
Risk	10	5	20	10	6.67
Risk	9	1	27	18	0.00

Table S2: Parameters and Data for Knowledge Treatment. "Gamble" and "Certain"
are dollar payoffs for the gamble and the certain payoff, respectively. "% Certain Choice"
is the percentage of fMRI subjects who chose the certain payoff rather than the gamble in
each row.

Condition	Question	Gamble	Certain	% Certain Choice
Ambiguity	The high temperature in Dushanbe, Tajikistan on November 7, 2003 was above 50 Fahrenheit.	15	6	43.75
Ambiguity	The high temperature in Tirana, Albania on March 19, 2002 was above 50 Fahrenheit.	23	6	6.25
Ambiguity	The high temperature in Rhodes, Greece on November 17 2003 was above 60 Fahrenheit.	18	9	43.75
Ambiguity	The high temperature in Hiroshima, Japan on November 17 2003 was above 50 Fahrenheit.	24	11	50.00
Ambiguity	Montpelier, VT. has the smallest population (2000 Census) amongst the state capitals.	21	10	68.75
Ambiguity	The population of the Mauritius (2003) is greater than 1 million.	18	11	68.75
Ambiguity	The population of Saskatchewan, Canada (2001 Census) is greater than 1 million.	15	6	25.00
Ambiguity	The population of Tallapoosa County, Alabama (2000 Census) is greater than 40,000.	20	6	12.50
Ambiguity	Andorra is bigger than Moldova	16	4	12.50
Ambiguity	Saint Kitts and Nevis is the smallest country in the Western Hemisphere?	19	6	18.75
Ambiguity	Lesotho is a larger (area) than Qatar.	18	6	18.75
Ambiguity	Burkina Faso is larger (area) than Guyana.	18	7	25.00
Ambiguity	The closing price of Paxar Corp on Nov 14, 2003 is above $15.	24	8	18.75
Ambiguity	The closing price of Cornell Companies on Nov 14, 2003 is above $10	16	6	31.25
Ambiguity	The closing price of Stride-Rite on Nov 14, 2003 is above $10	25	10	31.25
Ambiguity	The closing price of WhiteHall Jewelers on Nov 14, 2003 is above $10	22	7	6.25
Ambiguity	Ron Hunt was hit by a pitch more than 40 times in a season.	18	8	37.50

Ambiguity	Jumpin'' Joe Fulks was a 3 time All-Star between 1946 and 1954.	21	11	93.75
Ambiguity	Hal Bagwell holds the boxing record for most consecutive wins without a loss.	20	12	75.00
Ambiguity	Wesley Person was a second team all rookie.	25	13	93.75
Ambiguity	Marcantonio Raimondi was born in Siena.	25	7	6.25
Ambiguity	Ferdinand Bol painted Jacob's Dream	16	6	25.00
Ambiguity	Robert Clark was the real name of Robert Indiana.	25	8	12.50
Ambiguity	Georg Gross's middle name was Heinrich	25	10	12.50
Risk	The high temperature in New York City, NY on November 6, 2001 was above 60 Fahrenheit.	17	5	12.50
Risk	The high temperature in Los Angeles, California on November 16, 2001 was above 60 Fahrenheit.	25	10	6.25
Risk	The high temperature in San Francisco, California on November 16, 2001 was above 60 Fahrenheit.	21	7	12.50
Risk	The high temperature in Washington DC on November 16, 2001 was above 60 Fahrenheit.	19	8	31.25
Risk	The population of the United States (2000 census) is greater than 270 million.	18	13	43.75
Risk	The population of Texas (2000 census) is greater than 25 million.	19	9	37.50
Risk	The population of the New York City (2000 census) is greater than 8 million.	18	9	18.75
Risk	The population of Los Angeles County (2000 census) is greater than 10 million.	25	13	37.50
Risk	Michigan is larger (area) than Utah.	24	7	0.00
Risk	Arkansas is larger (area) than New York.	20	8	6.25
Risk	New Mexico is larger (area) than Arizona.	18	11	68.75
Risk	Georgia is larger (area) than Illinois.	17	5	18.75
Risk	The closing price of Microsoft on Nov 14, 2003 is above $25.	25	8	6.25
Risk	The closing price of IBM on Nov 14, 2003 is above $90.	15	6	25.00
Risk	The closing price of Coca-cola on Nov 14, 2003 is above $50.	22	11	68.75
Risk	The closing price of Ford Motors on Nov 14, 2003 is above $15.	20	6	6.25
Risk	Babe Ruth was born before 1900.	18	8	18.75
Risk	Michael Jordan played in more than	21	8	18.75

	1,200 games in the NBA			
Risk	Muhammad Ali won his first title after the 8th round.	15	6	18.75
Risk	Kobe Bryant's career high in points scored in a game is more than 60 points	22	11	37.50
Risk	Andy Warhol was Czech-American	17	8	25.00
Risk	Pablo Picasso's middle name was Ruiz	17	11	75.00
Risk	Rembrandt was born in Leiden	23	10	31.25
Risk	Michelangelo attended Seminary school	16	5	0.00

Table S3: Parameters for Informed Opponents Treatment. "# Total Cards" and "# Opponents Draw" are the number of cards in the ambiguous deck, and the number that an opponent drew, looked at, and replaced. "Gamble" and "Certain" are dollar payoffs for the gamble and the certain payoff, respectively. "% Certain Choice" is the percentage of fMRI subjects who chose the certain payoff rather than the gamble in each row. EV(binom) and EV(unif) are, respectively, the expected value of the gamble given a binomial or uniform prior over the composition of the deck (*S5*).

Condition	# Total Cards	# Opponents Draw	Gamble	Certain	% Certain Choice	EV (binom)	EV (unif)
Ambiguity	11	3	31	7	23.08	10.19	7.59
Ambiguity	18	3	36	6	0	11.25	8.00
Ambiguity	12	2	37	12	69.23	14.48	11.65
Ambiguity	17	3	30	8	84.62	10.84	8.15
Ambiguity	18	9	30	8	92.31	10.47	7.71
Ambiguity	10	5	36	15	84.62	14.81	11.87
Ambiguity	15	1	33	9	23.08	12.20	9.63
Ambiguity	13	5	29	5	38.46	8.70	6.16
Ambiguity	9	3	33	6	7.69	9.88	7.22
Ambiguity	14	3	33	6	0	10.37	7.48
Ambiguity	15	7	39	8	53.85	12.33	8.84
Ambiguity	3	1	33	7	7.69	9.00	7.17
Ambiguity	8	1	36	8	0	11.88	9.25
Ambiguity	6	3	39	9	46.15	11.81	9.05
Ambiguity	4	1	36	10	30.77	11.75	9.50
Ambiguity	16	7	30	5	38.46	8.97	6.25
Ambiguity	16	5	30	7	46.15	10.12	7.38
Ambiguity	11	4	28	8	84.62	10.05	7.69
Ambiguity	24	5	28	9	84.62	10.95	8.25
Ambiguity	19	5	35	11	100	13.39	10.11
Ambiguity	20	9	34	7	30.77	10.95	7.75
Ambiguity	9	3	30	5	30.77	8.75	6.33
Ambiguity	4	1	34	8	46.15	10.38	8.25
Ambiguity	11	4	29	5	38.46	8.76	6.32
Risk	24	0	24	6	0	9.00	9.00
Risk	7	0	28	10	15.38	12.00	12.00
Risk	7	0	21	6	0	8.25	8.25
Risk	10	0	22	8	7.69	9.50	9.50
Risk	21	0	18	11	76.92	10.00	10.00

Risk	12	0	28	11	7.69	12.50	12.50
Risk	19	0	22	10	46.15	10.50	10.50
Risk	6	0	24	11	30.77	11.50	11.50
Risk	12	0	23	7	0	9.25	9.25
Risk	8	0	26	10	7.69	11.50	11.50
Risk	17	0	18	9	84.62	9.00	9.00
Risk	12	0	25	7	0	9.75	9.75
Risk	19	0	26	8	0	10.50	10.50
Risk	18	0	24	9	0	10.50	10.50
Risk	17	0	22	10	53.85	10.50	10.50
Risk	7	0	28	8	0	11.00	11.00
Risk	8	0	23	9	0	10.25	10.25
Risk	13	0	22	8	0	9.50	9.50
Risk	24	0	18	7	15.38	8.00	8.00
Risk	25	0	21	10	92.31	10.25	10.25
Risk	8	0	22	5	0	8.00	8.00
Risk	6	0	26	9	7.69	11.00	11.00
Risk	17	0	26	13	84.62	13.00	13.00
Risk	12	0	21	8	15.38	9.25	9.25

Table S4: Summary of mean response times (secs) of choices across treatments.

Treatment	Ambiguity		Ambiguity Total	Risk		Risk Total	Grand Total
	Certain	Gamble		Certain	Gamble		
Card-Deck	4.88	5.67	5.30	8.45	6.30	7.13	6.22
Knowledge	7.53	8.29	8.03	6.03	7.32	6.98	7.51
Informed Opp.	5.39	5.93	5.69	5.40	3.54	3.96	4.83
Grand Total	5.83	6.80	6.39	7.00	5.80	6.16	6.27

Table S5: Summary of subject choices across treatment and condition. Average number of certain payoff choices by subjects across conditions and treatments (out of 24 total choices per condition per treatment).

Condition/Treatment	Card-Deck	Knowledge	Informed Opp.	Grand Total
Ambiguity	11.56	8.37	10.61	10.15
Risk	9.56	6.25	5.46	7.20
Ambiguity – Risk	2.00	2.12	5.15	2.95

Table S6: Ambiguity aversion estimates. Separate estimates (standard errors) of the ambiguity aversion coefficient γ, risk aversion coefficient ρ, and inflection parameter λ for subjects in the Card-Deck and Knowledge Conditions.

Subject	Card-Deck			Knowledge		
	γ	ρ	λ	γ	ρ	λ
AJB	0.98	1.00	1.39	1.11	1.13	0.71
	(0.10)	(0.09)	(0.63)	(0.15)	(0.12)	(0.41)
APS	0.80	0.90	4.32	1.66	1.44	0.10
	(0.04)	(0.04)	(1.92)	(0.57)	(0.48)	(0.18)
BIC	0.81	0.73	1.81	1.05	0.63	1.37
	(0.11)	(0.08)	(0.73)	(0.22)	(0.11)	(0.60)
BSU	1.20	0.73	9.98	1.09	1.07	0.51
	(0.10)	(0.04)	(4.82)	(0.19)	(0.15)	(0.34)
CSJ	0.93	0.87	3.85	1.30	1.50	0.10
	(0.07)	(0.04)	(1.50)	(0.46)	(0.71)	(0.26)
DAS	0.84	0.85	0.85	1.70	1.29	0.10
	(0.19)	(0.18)	(0.81)	(1.13)	(0.84)	(0.33)
EJH	0.82	0.83	1.39	1.09	1.05	0.64
	(0.12)	(0.10)	(0.67)	(0.17)	(0.13)	(0.39)
HCH	0.55	0.52	6.65	1.52	1.25	1.43
	(0.08)	(0.06)	(2.64)	(0.12)	(0.10)	(0.89)
KED	1.03	1.05	3.98	1.19	1.27	0.48
	(0.05)	(0.04)	(1.67)	(0.18)	(0.17)	(0.33)
LTL	0.98	1.02	0.80	1.07	0.89	2.13
	(0.15)	(0.14)	(0.55)	(0.09)	(0.05)	(0.78)
MK	1.12	1.01	0.85	1.30	1.37	0.10
	(0.16)	(0.13)	(0.52)	(0.45)	(0.55)	(0.21)
PRV	1.22	1.13	1.22	1.33	1.47	0.33
	(0.14)	(0.12)	(0.69)	(0.23)	(0.22)	(0.26)
SWT	0.81	0.58	5.01	1.10	0.70	10.16
	(0.09)	(0.05)	(1.56)	(0.06)	(0.03)	(3.77)
TEJ	0.84	0.79	5.35	1.49	1.36	0.26
	(0.06)	(0.03)	(1.83)	(0.26)	(0.22)	(0.21)
VS	1.19	1.22	0.63	1.42	1.50	0.15
	(0.19)	(0.18)	(0.51)	(0.27)	(0.26)	(0.14)
WL	0.85	0.83	1.11	1.88	1.38	0.18
	(0.13)	(0.10)	(0.59)	(0.41)	(0.27)	(0.18)
Mean est.	0.94	0.88	3.07	1.33	1.21	1.17
Mean s.e.	(0.11)	(0.09)	(1.35)	(0.31)	(0.28)	(0.58)

Table S7: *Ambiguity > Risk* regions. Local maxima of clusters, $p < 0.001$ uncorrected, clusters with $k < 10$ voxels not shown (All local maxima uncorrected p-values are significant to three significant figures, and are omitted from the table.)

cluster			voxel							Regions	
p_{cor}[1]	k_E[2]	p_{unc}[3]	p_{FWE}[4]	p_{FDR}[5]	T[6]	Z[7]	X[8]	Y	Z	L/R[9]	Region
0.01	82	0.001	0.011	0.007	5.96	5.04	51	33	-6	R	Lateral Orbitofrontal Cortex
			0.897	0.017	3.92	3.6	54	18	-21		
0	109	0	0.052	0.007	5.38	4.67	-54	-60	42	L	Inferior Parietal Lobule
			0.1	0.007	5.13	4.5	-45	-54	33		
0	112	0	0.06	0.007	5.33	4.63	-9	48	39	L	Dorsomedial Prefrontal Cortex
			0.306	0.008	4.66	4.16	-12	63	21		
0	119	0	0.072	0.007	5.26	4.59	54	-54	36	R	Supramarginal Gyrus
			0.599	0.01	4.3	3.89	54	-63	30		
0	226	0	0.162	0.007	4.94	4.36	18	54	18	R	Dorsomedial Prefrontal Cortex
			0.229	0.008	4.79	4.26	12	54	30		
			0.379	0.009	4.56	4.09	12	27	57		
0.06	52	0.007	0.201	0.008	4.85	4.3	36	18	42	R	Middle Frontal Gyrus
			0.884	0.016	3.94	3.62	42	9	45		
0	154	0	0.22	0.008	4.81	4.27	60	-36	-3	R	Middle Temporal Gyrus
			0.485	0.009	4.43	3.99	63	-27	-6		
			0.626	0.01	4.27	3.87	51	-24	-9		
0.44	21	0.066	0.302	0.008	4.67	4.17	-39	-9	-15	L	Sub-Gyral
0.13	40	0.015	0.331	0.009	4.63	4.14	39	6	-27	R	Frontoinsular Cortex
			0.951	0.019	3.8	3.5	42	15	-24		
0.41	22	0.061	0.547	0.01	4.36	3.94	54	27	6		Lateral Orbitofrontal Cortex
0.26	29	0.034	0.584	0.01	4.32	3.91	-54	36	-6	L	Lateral Orbitofrontal Cortex
0.74	12	0.154	0.75	0.013	4.13	3.76	-15	-15	-15	L	Amygdala/Parahippocampal Gyrus
			0.993	0.026	3.57	3.32	-21	-6	-18	L	Amygdala
0.41	22	0.061	0.825	0.014	4.03	3.69	33	-6	-27	R	Amygdala/Parahippocampal Gyrus

---

[1] Corrected (family-wise) cluster-level p-value.
[2] Cluster size (voxels).
[3] Uncorrected cluster-level p-value.
[4] Corrected (family-wise) voxel-level p-value.
[5] Corrected (false-discovery rate) voxel-level p-value.
[6] T-statistic of voxel.
[7] Z-score of voxel.
[8] (X, Y, Z) are the MNI coordinate of voxel location (mm).
[9] Laterality (L = left, R = right).

Table S8: *Risk>Ambiguity* regions. Local maxima of clusters, $p < 0.001$ uncorrected, clusters with $k < 10$ voxels not shown (All local maxima uncorrected p-values are significant to three significant figures, and are omitted from the table.)

cluster			voxel							Regions	
p_{cor}	k_E	p_{unc}	p_{FWE}	p_{FDR}	T	Z	X	Y	Z	L/R	Region
0.06	52	0.007	0.063	0.012	5.31	4.62	0	-6	6	M	Caudate
			0.993	0.033	3.57	3.32	9	6	6	R	
			0.952	0.023	3.79	3.5	-12	6	0	L	
0	641	0	0.07	0.012	5.27	4.59	12	-60	-3	R	Culmen
			0.119	0.012	5.07	4.45	9	-78	3	R	Lingual Gyrus
			0.162	0.012	4.94	4.36	-12	-75	15	L	Cuneus
0.01	81	0.001	0.295	0.012	4.68	4.18	-15	-72	51	L	Precuneus
0.26	29	0.034	0.338	0.012	4.62	4.13	-3	9	45	L	Precentral Gyrus
0.12	41	0.014	0.569	0.012	4.33	3.92	12	-75	51	R	Precuneus
			0.906	0.02	3.9	3.58	21	-84	39		
0.74	12	0.154	0.923	0.021	3.87	3.56	-42	-75	30	L	Angular Gyrus

Table S9: *Gamble>Certain* regions: Local maxima of clusters, $p < 0.001$ uncorrected, clusters with $k < 10$ voxels not shown (All local maxima uncorrected).

cluster			voxel								Regions	
p_{cor}	k_E	p_{unc}	p_{FWE}	p_{FDR}	T	Z	p_{unc}	X	Y	Z	L/R	Region
0	129	0	0.01	0.005	5.47	5.04	0	18	-78	-12	R	Occipital Cortex
			0.998	0.121	3.37	3.26	0.001	0	-81	-3		
0.037	54	0.004	0.398	0.041	4.31	4.09	0	-9	-21	48	L	Medial Frontal Gyrus
			0.609	0.057	4.1	3.91	0	-18	-12	51	L	Brodman Area 6
0.122	37	0.013	0.781	0.072	3.93	3.76	0	-30	-27	54	L	Precentral Gyrus
0.639	14	0.104	0.88	0.088	3.81	3.65	0	-33	15	21	L	Insula
0.76	11	0.146	0.891	0.089	3.8	3.64	0	-6	15	-3	L	Caudate head
0.72	12	0.13	0.947	0.095	3.69	3.54	0	15	-90	12	R	BrodmanArea18
0.72	12	0.13	0.982	0.104	3.57	3.43	0	33	6	21	R	Insula
			0.999	0.124	3.33	3.21	0.001	27	12	21		
0.562	16	0.084	0.997	0.12	3.41	3.29	0	-51	-66	6	L	Middle Temporal Gyrus
			0.999	0.124	3.33	3.21	0.001	-51	-57	3		

Table S10: *Certain>Gamble* regions: Local maxima of clusters, $p < 0.001$ uncorrected, clusters with $k < 10$ voxels not shown (All local maxima uncorrected).

cluster			voxel								Regions	
p_{cor}	k_E	p_{unc}	p_{FWE}	p_{FDR}	T	Z	p_{unc}	X	Y	Z	L/R	Region
0.001	122	0	0.008	0.003	5.56	5.11	0	42	-24	60	R	Precentral Gyrus
0.012	72	0.001	0.008	0.003	5.56	5.11	0	-15	-75	9	L	Occipital Cortex

Table S11: Regions positively correlated with expected value of decisions in risk condition of Card-Deck treatment. Local maxima of clusters, $p < 0.005$ uncorrected, clusters with $k < 10$ voxels not shown (All local maxima uncorrected).

cluster			voxel								Regions	
p_{cor}	k_E	p_{unc}	p_{FWE}	p_{FDR}	T	Z	p_{unc}	X	Y	Z	L/R	Region
0.002	120	0	0.089	0.089	7.11	4.64	0	9	24	54	R	Superior Frontal Gyrus
			0.994	0.397	4.85	3.71	0	12	39	51		
			1	0.397	4.47	3.51	0	9	12	54		
0.429	36	0.01	0.32	0.16	6.36	4.36	0	60	-33	3	R	Middle Temporal Gyrus
			1	0.397	3.31	2.82	0.002	57	-42	3		
0.844	23	0.032	0.781	0.314	5.76	4.12	0	-51	-72	30	L	Angular Gyrus
			1	0.397	3.99	3.24	0.001	-42	-78	33		
1	10	0.139	0.991	0.397	4.92	3.74	0	-66	-30	-9	L	Middle Temporal Gyrus
0.487	34	0.012	0.996	0.397	4.81	3.68	0	-9	-18	18		
			1	0.397	4.16	3.34	0	-9	-3	18		
0.403	37	0.009	1	0.397	4.55	3.55	0	15	6	3	R	Caudate
0.041	70	0.001	1	0.397	4.37	3.46	0	48	24	-15	R	Inferior Frontal Gyrus
			1	0.397	3.67	3.05	0.001	54	39	-3	R	Brodman Area 47
			1	0.397	3.54	2.97	0.001	39	24	-15		
0.783	25	0.026	1	0.397	4.21	3.37	0	-9	45	9	L	Anterior Cingular Gyrus
0.549	32	0.014	1	0.397	3.99	3.24	0.001	-3	57	33	L	Brodman Area 9
			1	0.397	3.87	3.17	0.001	-9	39	30		
			1	0.397	3.46	2.92	0.002	-6	48	27		
0.999	11	0.122	1	0.397	3.95	3.22	0.001	3	-42	-6	M	Culmen
0.897	21	0.039	1	0.397	3.85	3.16	0.001	60	-57	30	R	Supramarginal Gyrus
			1	0.397	3.73	3.09	0.001	60	-51	39		
0.999	11	0.122	1	0.397	3.84	3.16	0.001	-6	27	42	L	Brodman Area 6
1	10	0.139	1	0.397	3.74	3.1	0.001	-45	42	6	L	Inferior Frontal Gyrus
1	10	0.139	1	0.397	3.43	2.9	0.002	21	48	27	R	Superior Frontal Gyrus
			1	0.397	3.38	2.87	0.002	18	57	33		

Table S12: Regions positively correlated with expected value of decisions in Knowledge treatment. Local maxima of clusters, $p < 0.005$ uncorrected, clusters with $k<10$ voxels not shown (All local maxima uncorrected).

cluster			voxel								region	
p_{cor}	k_E	p_{unc}	p_{FWE}	p_{FDR}	T	Z	p_{unc}	X	Y	Z	L/R	Region
0.782	41	0.06	0.417	0.741	5.88	4.17	0	33	-87	15	R	Middle Occipital Gyrus
			1	0.93	3.53	2.96	0.002	39	-84	9		
0.995	17	0.21	0.998	0.93	4.08	3.3	0	-9	12	3	L	Caudate
			1	0.93	3.24	2.78	0.003	-6	3	6		
1	10	0.334	1	0.93	3.69	3.06	0.001	-24	-63	51	L	Superior Parietal Lobule

Table S13: Cross correlation (*p*-values) of pooled contrast values (each subject contributes one data point) between regions (ambiguity-risk contrast for amygdala and OFC; risk-ambiguity contrast for dorsal striatum). Note that since the contrasts are opposite for amygdala-OFC and striatum, positive correlations actually represents negative correlation in activity.

	R Amyg	L Amyg	R OFC	L OFC	R DMPFC	R DMPFC	R DStr	L DStr
R Amyg	-							
L Amyg	0.33 (0.21)	-						
R OFC	0.22 (0.42)	0.00 (0.99)	-					
L OFC	0.03 (0.91)	0.15 (0.58)	0.38 (0.14)	-				
R DMPFC	0.35 (0.18)	-0.10 (0.73)	0.76 (0.00)	0.58 (0.02)	-			
R DMPFC	0.23 (0.38)	0.12 (0.65)	0.46 (0.07)	0.09 (0.73)	0.56 (0.03)	-		
R DStr	-0.11 (0.69)	0.00 (1.00)	0.13 (0.63)	0.31 (0.24)	0.24 (0.37)	-0.31 (0.24)	-	
L DStr	-0.22 (0.40)	-0.16 (0.55)	0.14 (0.59)	0.61 (0.01)	0.08 (0.76)	-0.31 (0.24)	0.33 (0.22)	-

Table S14: Summary of lesion patient choices. Proportion of patients choosing certain amount x when choosing between a gamble for 0 or 100 points versus x. In the ambiguity condition, the deck is of unknown composition of red and black cards. In the risk condition, the deck is known to contain 50 red cards and 50 black cards. Higher proportion of certain choices suggests greater risk/ambiguity aversion. A population of deterministic risk-neutral subjects would have proportions of 0, 0, 0, 0, 1.

Lesion	Certain Amt	Ambiguity	Risk
Control	15	0.2857	0
	25	0.2857	0.1429
	30	0.5714	0.2857
	40	0.7143	0.5714
	60	0.7143	0.8571
OFC	15	0	0
	25	0	0
	30	0	0
	40	0.2	0.2
	60	0.4	0.6

Table S15: Lesion patient performance measures: Means (standard deviations) of VIQ, PIQ, FSIQ: verbal performance and full scale IQ from the Wechsler Adult Intelligence Test III or Revised. MATH: from the WRAT-R arithmetic subtest. MEMORY: from the Wechsler Memory Scale 3, general memory index. WCST: Wisconsin card sorting task (number of categories successfully sorted).

	OFC	Control	t-statistic
Age	54	52	0.31
	(12)	(9)	
VIQ	110	100	1.00
	(21)	(9)	
PIQ	117	100	2.35
	(11)	(14)	
FSIQ	114	100	1.65
	(17)	(10)	
MATH	102	98	0.71
	(10)	(9)	
WCST	6	4.9	1.45
	(0)	(2)	
MEMORY	106	100	1.09
	(7)	(12)	

Supplementary References

S1.   The constraint of $\gamma = 1$ for the risk condition is not necessary in the Card-Deck treatment, as the probabilities in the risk condition are well defined and varied. In both the Knowledge and Informed Opponents treatments, however, <u>all</u> probabilities are assumed to be ½. Allowing probability weighting in the risk condition renders the models under-identified. Furthermore, in the Card-Deck treatment, allowing γ_{risk} to vary, and treating the ratio $\gamma_{amb}/\gamma_{risk}$ as the measure of ambiguity aversion (the constrained case is equivalent to $\gamma_{amb}/1$), leads to nearly identical estimates, with a correlation of 0.98 across subjects between the constrained and unconstrained estimates. Allowing non-linear weighting of probabilities in the form of $w(p) = 1/exp(-ln(p)^{\alpha})$ suggested in S2, also yields similar results, $\rho = 0.86$.

S2.   D. Prelec, *Econometrica* **66**, 497 (1998).

S3.   J. Nelder, R. Mead, *Comput. J.* **7**, 308 (1965).

S4.   University College London, *Statistical Parametric Mapping*. Information available at http://www.fil.ion.ac.uk.

S5.   We performed a separate conjunction analysis at the second level. As the conjunction is a test on the minimum statistic, it may therefore be a better control for the biases that may be produced through an ANOVA (*S6*). The regions found active in the conjunction analysis were qualitatively similar to those found with the present method.

S6.   K. Friston, W. Penny, D. Glaser, *NeuroImage* **25**, 661 (2005).

S7. M. Paulus, et. al. *NeuroImage* **19**, 1085 (2003).

S8. To calculate the expected value of the gamble in the Informed Opponents treatment, we solve first the optimal strategy of the opponent. Denote (N,R,n,r) as respectively the number of cards total in the deck, the number of red cards total in the deck, the number of cards in the sample the opponent observes, and the number of red cards in the sample the opponent observes.

The opponent knows (N,n,r). His optimal strategy is therefore simply to choose the more likely color in the deck given the realizations of his sample. That is, the opponent chooses according to $\max\left(\dfrac{E(R\,|\,r,n,N)}{N},1-\dfrac{E(R\,|\,r,n,N)}{N}\right)$. The only unknown in the expression is the numerator. To solve, apply Bayes' rule, such that $P(R\,|\,r,n,N) = \dfrac{P(R\,|\,N)P(r\,|\,R,n,N)}{\displaystyle\sum_{i=0}^{N}P(r\,|\,i,n,N)}$, where $P(R\,|\,N)$ is the prior distribution on R, $P(r\,|\,R,n,N)$ is the hypergeometric distribution (as this is an example of sampling without replacement), and the denominator is the probability of observing r over the support of R. With $P(R\,|\,r,n,N)$ in hand, the opponent can calculate the expected number of red cards in the deck, which is

$$E(R\,|\,r,n,N) = \sum_{R=0}^{N}P(R\,|\,r,n,N)\times R.$$

Because this is a constant-sum game, the subject's probability of winning is the expected proportion of color that the subject is betting on in the deck $P(win\,|\,r,n,N) = \min\left(\dfrac{E(R\,|\,r,n,N)}{N},1-\dfrac{E(R\,|\,r,n,N)}{N}\right)$. That is, the complement of

the opponent's. As the subject does not observe r, we need to take the expecation

over r. That is, $P(win \mid n, N) = \sum_{r=0}^{n} P(r \mid n, N) \times P(win \mid r, n, N)$.

Given the independence of the choices of the subject and the opponent, their choices will coincide with $p = 0.5$ in expectation. In this case, according to the rules of the game, the bet does not take place and both earn the certain payoff. The payoff function for the subject is therefore $0.5 \times P(win \mid n, N) \times x + 0.5 \times c$, where x is the amount of the gamble, and c is the certain payoff.

Finally, note that the choice of priors $P(R|N)$ is left unspecified in the above. For example, if the subject believes that the deck is composed of either all red cards or all blue cards ($P(R=N|N)=0.5$ and $P(R=0|N)=0.5$), a sample from the deck would determine completely the composition of the deck. We present in Table S3 expected value calculations given a uniform prior— $P(R \mid N) = 1/N + 1, \forall R$, and a

binomial prior with $p = \frac{1}{2}$— $P(R \mid N) = \binom{N}{R} \left(\frac{1}{2}\right)^{R} \left(\frac{1}{2}\right)^{N-R}$.

S9. S. Mukerji, J.-M. Tallon, *Uncertainty in Economic Theory: A collection of essays in honor of David Schmeidler's 65th Birthday*, I. Gilboa, ed. (Routledge, London, 2004).

S10. L. Hansen, T. Sargent, *Amer. Econ. Rev.* **91**, 60 (2001).

S11. T. Bewley, *Decisions in Economics and Finance* **25**, 79 (2002).

S12. S. Mukerji, *Amer. Econ. Rev.* **88**, 1207 (1998).

S13. K. C. Lo, *Games and Econ. Behavior* **28**, 256 (1999).

S14. C. Camerer, R. Karjalainen, *Models and Experiments on Risk and Rationality* , B. Munier, M. Machina, eds. (Kluwer Academic Publishers, Dordrecht, 1994), pp. 325–358.

S15. P. Ghirardato, J. Katz, *J. Pub. Econ. Theory,* in press.

S16. J. Dow, S. R. da Costa Werlang, *Econometrica* **60**, 197 (1991).

S17. L. Epstein, T. Wang, *Econometrica* **62**, 283 (1994).

S18. P. Duff, *Law and Contemporary Problems* **62**, 173 (1999).

S19. K. French, J. Poterba, *Amer. Econ. Rev.* **81**, 222 (1991).

S20. J. Siegel, *Stocks for the Long Run* (Irwin, New York, ed. 2, 1998).

S21. J. Graham, H. Campbel, H. Han. Undated. Working paper.

http://ideas.repec.org/p/nbr/nberwo/11426.html

1 Instructions

This is an experiment on decision making. If you follow the instructions and make good decisions you could earn a significant amount of money. The experiment will consist of three *rounds*. Each round consists of a sequence of *choices*. In each choice, you choose between a sure amount of money and a gamble which pays an amount of money that depends on a draw of a card, or an event which happened. At the end of the experiment, one of the choices from each round will be chosen at random by drawing a numbered card from a deck. If the number 12 is chosen, for example, then the 12th choice will be used to determine your payment for that round. If you chose the sure amount in that round, you will earn that sure amount. If you chose the gamble in that round, the gamble will be played (or you will be told which event happened), which will determine how much money you earn. There will be 3 rounds.

2 Round 1

In this round you will make a series of choices between a gamble with an uncertain payoff, and a certain payoff. A sample screen is as follows
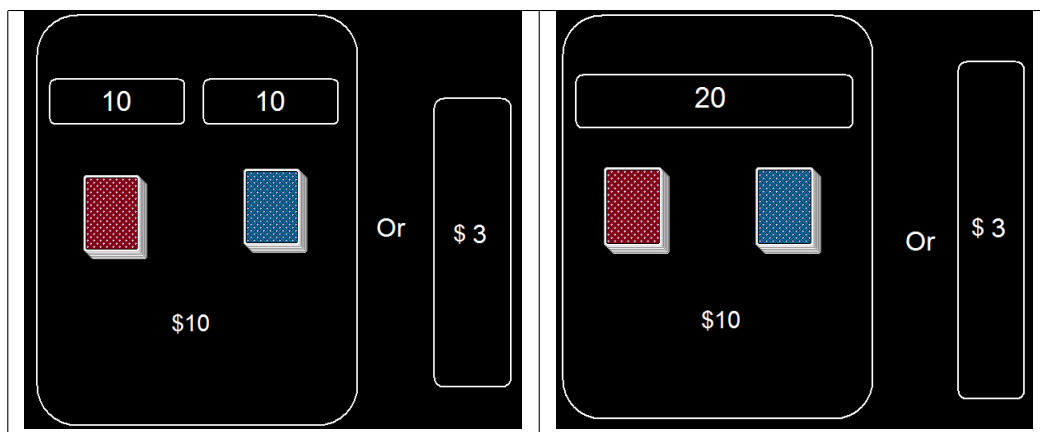
The numbers in the box on top of the cards show the number of cards in a deck. In the example on the left there are 10 red cards and 10 blue cards. The dollar amount underneath the cards shows the amount you earn if the color you choose is the same as the color of the card which is actually drawn, at the end of the experiment. In the example on the left you would earn $10 if you choose the gamble, and choose the correct card color, and you would earn $3 if you choose the sure amount on the right.

Sometimes you will not know the exact numbers of cards of different colors. Instead, you will only know the *total* number of cards; you will not know how many cards are of each color. The example screen on the right shows this

situation. The box at the top of the screen shows that there are a total of 20 cards, but you do not know how many red or blue cards there are.

In each choice in this round, you should choose between the red card, blue card, or certain payoff. At the end of experiment, one of these trials will be selected at random and played for money. If you chose the gamble, the gamble will be played with a deck of cards. Suppose that the screen on the left was chosen. There will then be 10 red cards and 10 blue cards (you may verify this). A random card will be chosen. If your choice in that round matches the card chosen, you will earn $10. If your choice is the opposite of the actual card color chosen, you earn $0.

Suppose that the screen on the right was chosen. There will be 20 cards of either blue or red cards (you can verify the composition afterwards). A random card will be chosen. If your choice in that round matches the card chosen, you will earn $10. If your choice is the opposite of the actual card color chosen, you earn $0.

If you chose the certain outcome in the examples above, you will earn $3.

Note that the numbers of cards, and the dollar amounts you can earn, will be different in different choices within the round.

3 Round 2

In this round you will also choose between answering "Yes" or "No" to a knowledge question, which pays a dollar amount if your answer is correct, and receiving a certain payoff. Here is a sample screen:

At the end of the experiment, one of the choices in this round will also be selected at random and played. If you choose to answer the knowledge question, you will be paid according to whether your answer is correct. In the choice

above, the correct answer is "No". You would earn $10 if you answered No, and $0 if you answered Yes.

If you chose the certain outcome, you will receive $3.

4   Round 3

The choices in round 3 are similar to those in round 1, because they involve red and blue cards. However, in the choices in this round you will be competing with another person. The other person will draw a batch of cards at random, look at the color of the cards, and return them to the deck. A number at the top of the screen will tell you how many cards your opponent has drawn. In the example screen below, your opponent will draw a group of 3 cards, all at once. In this example, there are 20 cards which are red and black, but you do not know how many cards of each color there are. Since your opponent will have drawn a batch of three cards, the opponent may have a better idea of the number of cards of each color than you do.

After your opponent has seen the colors of the cards in the batch, and returned the cards to the deck, your opponent will choose whether to bet on red or blue. If you choose to bet on red or blue, rather than take the certain amount on the right side of the screen, then your bet will only take place if the opponent chose the *opposite* color to the one you chose. For the sample screen above, suppose your opponent saw a batch of 3 cards and then chose "red". If you choose red as well, then the bet will not take place because you chose the same color as your opponent did. Then you will both earn the certain amount of $3 instead. If you choose the opposite color of your opponent– blue, in this example– then the bet will take place. Then you earn $15 if the actual card chosen is blue, and you earn $0 if the actual card chosen is red.

5   Review

The experiment consists of three (3) rounds. Within each round, you will be making several choices. The questions in each round have different numbers of red and blue cards, or different knowledge questions, and different money payoffs. are different. At the end of the round, you will randomly choose an index card from a numbered deck. The number on the card will determine which choice will be used to determine your payment. Three numbers will be chosen, one for each of the three rounds.

In the first round, in each choice you will either play a gamble by drawing a card out of a deck, or receive a fixed payment. The card deck's composition and monetary payoff is specified on the screen. In the second round, you will either play a gamble by answering a knowledge question or receive a fixed payment. In the third round, you will play against an opponent who will draw a number of cards from the deck, look at them, then return them to the deck If you choose a card color, your bet will only count if the opponent chooses the *opposite* color.

6   Quiz

1. If I choose red in round 1, and a blue card is drawn, I earn $0 in that choice. (circle one)   True   False

2. In round 3, another person will see a batch of cards that I will not see. (circle one)   True   False

3. In round 3, if the opponent chooses the *same* color as I did, the bet will still take place   (circle one)   True   False